Test results, their interpretation and application

I 7

Test Results, their Interpretation and Application.

Versuche, Ausdeutung und Anwendung der Ergebnisse.

Essais; signification et application des résultats.

Dr. Ing. H. Maier-Leibnitz,
Professor an der Technischen Hochschule Stuttgart.

A. Simply supported full-web beams (plated beams).

In order to be able to interpret the test results of continuous beams, the behaviour of a simply supported beam of span l, carrying a point load P in mid-span shall be explained first. (Fig. 1, see [1].)[1] For this purpose an I-beam 14 cm · 14 cm was used and the following properties were found by measuring the actual cross section: Sectional area: $F = 43.2\ cm^2$; moment of

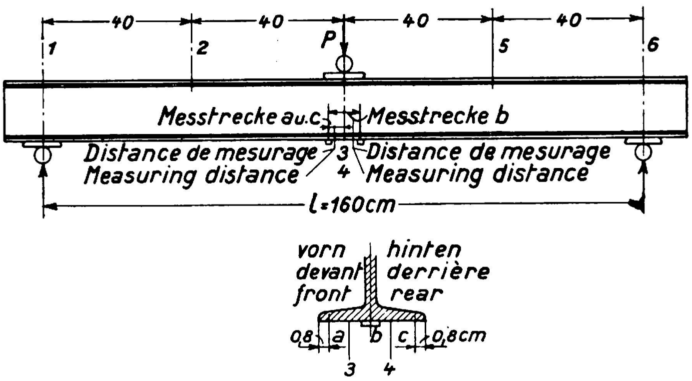

Fig. 1.

inertia $J = 1525\ cm^4$; modulus of section $W = 214\ cm^3$. Four test pieces cut from the flanges of this joist gave an average yield point stress of $\sigma_s = 2.437\ t/cm^2$. In Fig. 2 are shown the total and permanent deflections in mid-span and in Fig. 3 the average values of total and permanent elongations and straining at the points a and c of the bottom flange in mid-span. During the execution of tests it was noticed that scaling occurred in mid-span on the underside of the compression flange for a point load of $P = 12.8\ t$ For a load $P_v = 17.15\ t$ the beam buckled sideways, leading to complete failure.

The term *carrying capacity* of a beam can be interpreted variously. Based on the assumption that a beam is of no further use if it begins to have permanent deformations, this *carrying capacity* $[P_T]$ could be expressed

[1] The numbers given in [ ]-brackets refer to publications listed at the end.

as the value of P for which the extreme fibres at the point of max. bending moment are stressed up to yield point. If the load P is only slightly increased,

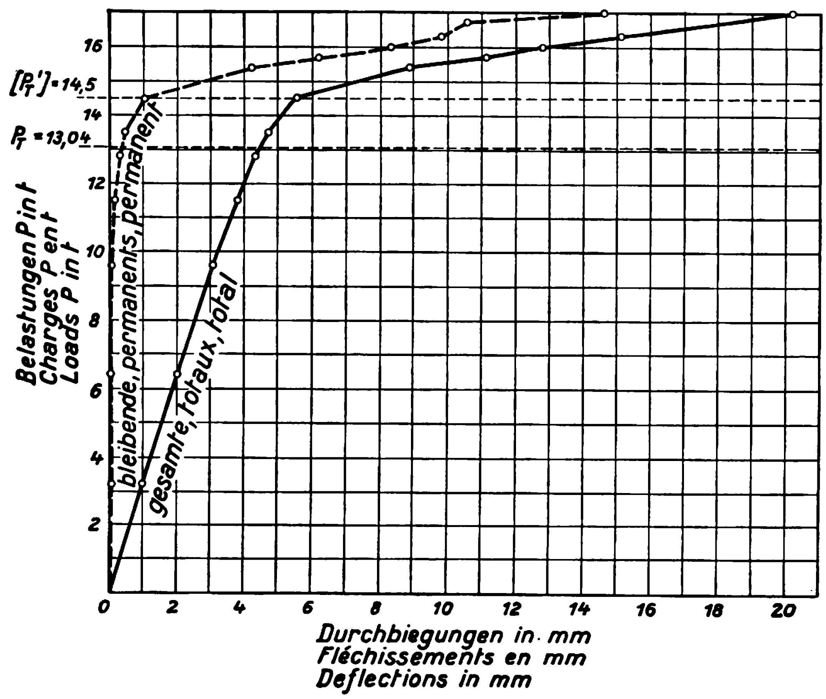

Fig. 2. Beam 11 a, mean of deflections for points 3, 4 in mid-span.

permanent deformations and deflections would occur. The corresponding bending moment is in this case of the following value:

$$M_s = W \cdot \sigma_s = 214 \cdot 2.437 \text{ cmt},$$

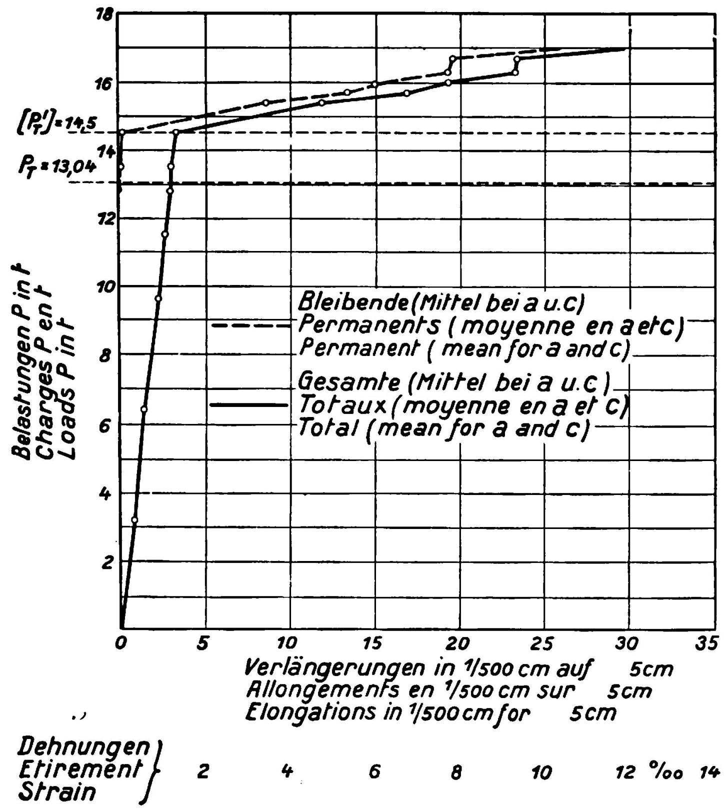

Fig. 3. Beam 11 a.

giving a carrying capacity of

$$[P_T] = \frac{4 \cdot W \cdot \sigma_s}{l} = 13.04\,t.$$

From Fig. 3 it can be seen that permanent straining really starts with this load.

Attempts have often been made to arrive analytically at the value of M'_s, of the *carrying moment* which ultimate value cannot be exceeded and which corresponds to the internal moment of the stresses after yielding and for complete plasticity of the whole cross section. (See, e.g. [2], [3], [4], [5], further references to publications are given in [5] concerning the analytical method of *Prager* and *Kuntze*). As shown in the report by *Fritsche* [5], numerical conformity between experiment and calculation cannot be expected (the cross sections do not remain even as plasticity increases; the values of yield stresses vary for different points along the flange; hardening of the material due to yield).

From Fig. 3 and also from Fig. 2 relating to the tests under consideration, the value $[P'_T] = 14{,}5$ t, corresponding to M'_s, can be measured distinctly, after which permanent deformations and deflections develop at the bottom flange at the point of attack of the load and increase almost unrestrictedly. The corresponding *carrying moment* for this load has the value:

$$M'_s = \frac{[P'_T] \cdot l}{4} = 580 \text{ cmt. (See also section D a)}$$ [2]

The ratio $\frac{[P'_T]}{[P_T]} = \frac{14.5}{13.04} = 1.10$

applies for the present case.

The tests published in [1] for loading according to Fig. 1 give ratios as under:

$$\text{I-beam Burbach } \frac{152}{127} : \frac{[P'_T]}{[P_T]} = \frac{14.7}{12.66} = 1.16,$$

$$\text{I-beam 16: } \frac{[P'_T]}{[P_T]} = \frac{8.3}{7.61} = 1.09$$

In any case, as already shown by *Grüning* in [2] it does not appear justifiable to consider the quantities P_v and P_w (in the treatise of *Stüssi-Kollbrunner* [6]) as being decisive for the carrying capacity, or even to regard these values as the carrying capacity of beams.

For a clear conception (qualitative interpretation), concerning the tests described in sections B to E for continuous and fixed beams, and for the purpose of establishing a simple mode of calculation for such beams, it appears important to understand fully that the relation between the *permanent* deflection f of a beam AB (and similarly the residual angle φ of the deflection curve) and the load P or the bending moment $\frac{P \cdot l}{4}$ (see Fig. 4a) can be expressed by the curve OCDE in Fig. 4b (identical with Fig. 5 in [1]). To render the above

[2] If a curve were to replace the straight lines in Fig. 2 and 3 the value of $[P'_T]$ would be read as 15 t in which case $M'_s = 600$ cmt.

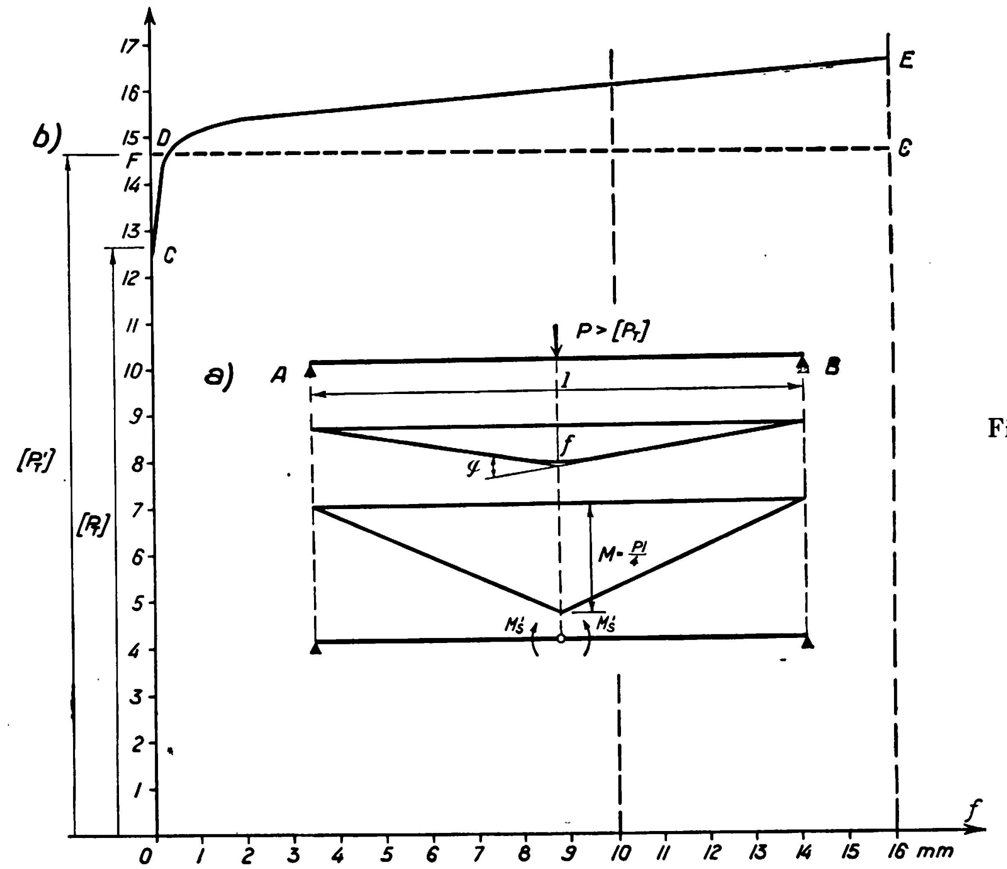

Fig. 4.

still easier to understand, the curve CDE can be replaced by a horizontal line F G and the permanently bent beam can be considered to have a sharp kink at the middle of the span (Fig. 4a). In this case we get

$$\varphi = \frac{2 \cdot f}{\frac{l}{2}} \quad \text{or} \quad f = \frac{\varphi \cdot l}{4}$$

The simplified conception of the problem leads to the assumption that the beam would not be capable of withstanding a higher moment than $M'_s = \frac{[P'_T] \cdot l}{4}$ (in this in particular case $M'_s = 580$ cmt) and that under this moment the beam is bent with a sharp kink at the load point. This is equivalent to the conception of a beam loaded with $[P'_T]$ being hinged at the point of attack of the load, the hinge being equipped with an internal moment maintaining equilibrium with the bending moment M'_s.

Further tests with simply supported beams can be found in [7], [8], [9], [10], [15].

B. Continuous beams of two spans and equal loading for both spans.

Fig. 5 shows the results of tests carried out by the Author with two compound I-beams with a depth of 16 cm, described in [11]. Four different cases were studied and the values P_{zul} of the permissible loads are given, for which

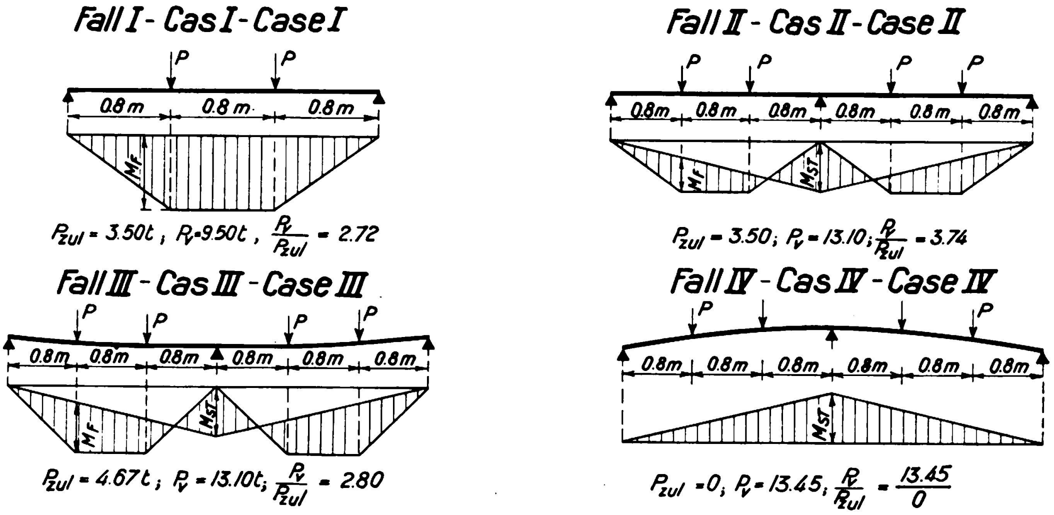

Fig. 5.

according to the usual theory of elasticity the permissible stress $\sigma_{zul} = 1.2$ t/cm² is attained.

Case I is that of a simply supported beam over one span, Case II a continuous beam over two spans with bearings all at the same level. Case III treats a continuous beam over two spans with the intermediate support lowered in such a way as to produce a bending moment over the central support equal in value to the maximum moment in the span, but being equal to the permissible bending moment: $W \cdot \sigma_{zul}$. Case IV has the following characteristics: continuous beam over two spans, but with the end supports at a lower level than for the intermediate support, in such a way as to establish a moment over the middle support equal to the permissible moment $W \cdot \sigma_{zul}$.

Failure of all beams occurred for the loads P_v after the production of unreasonably high deformations, by lateral buckling in the vicinity of the outer

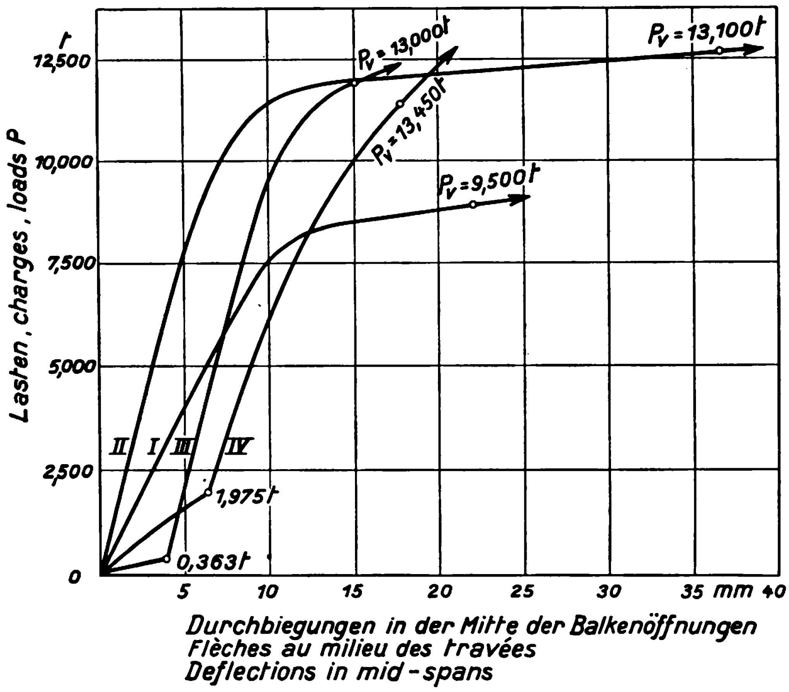

Fig. 6.

forces. The deflections registered for the middle of the spans are given in Fig. 6.

In case I the first traces of yielding were observed at the tension flange under the point of attack of the load for $[P'_T] = 7.5$ t, giving a stress of $2.70\ t/cm^2$, which is less than the average yield point stress of $2.94\ t/cm^2$ as determined by tensile tests. Based on observations made with these tests, it can be assumed that $[P'_T] = 8.5$ t,[3] giving a corresponding carrying moment of $M'_s = 8.5 \cdot 80 = 680$ cmt. The modulus of section for the two compound I-beams is $W = 222\ cm^3$. With this value and for $\sigma_s = 2.70\ t/cm^2$ we receive a moment of $M_s = W \cdot \sigma_s = 222 \cdot 2.70 = 600$ cmt or correspondingly for $\sigma_s = 2.94\ t/cm^2$ a moment of $M_s = 222 \cdot 2.94 = 665$ cmt. For $\frac{[P'_T]}{[P_T]} = 1.14$ the following ratios are received:

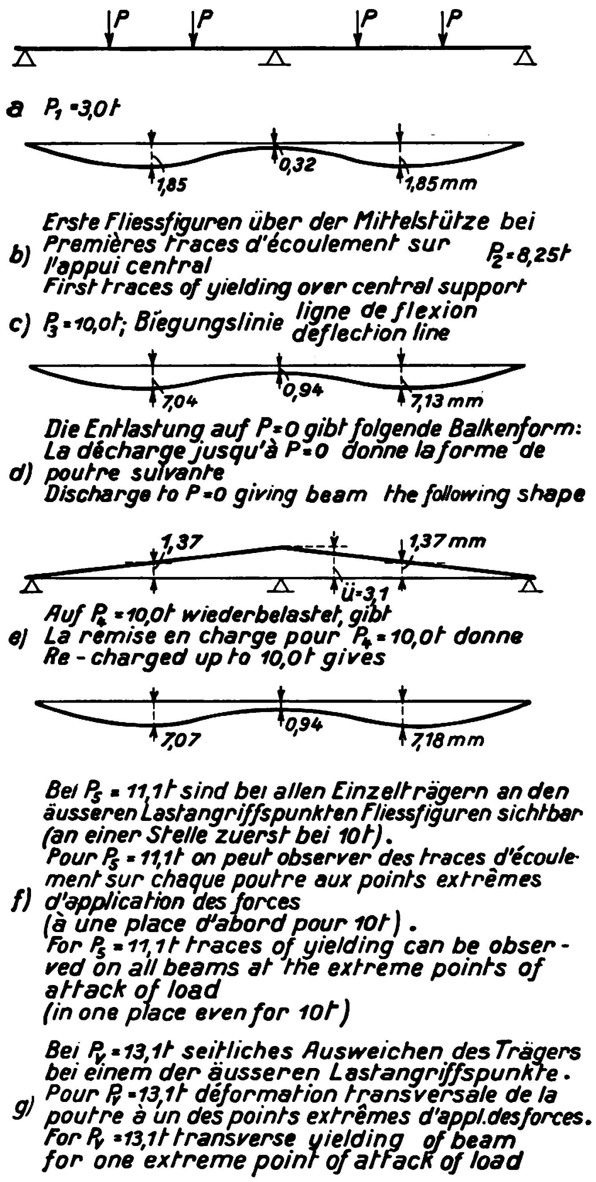

Fig. 7.

Diagram showing principal test II.

[3] The values for carrying capacity of simply supported beams are marked thus: [ ]; $[P_T]$ and $[P'_T]$ refer throughout to the simply supported single span reference beam.

$\frac{M'_s}{M_s} = \frac{680}{600} = 1.14$ in one case and $\frac{680}{665} = 1.02$ in the other case. These results show that it is impossible to deduce the bending moment M'_s from the yield stress received by tensile tests.

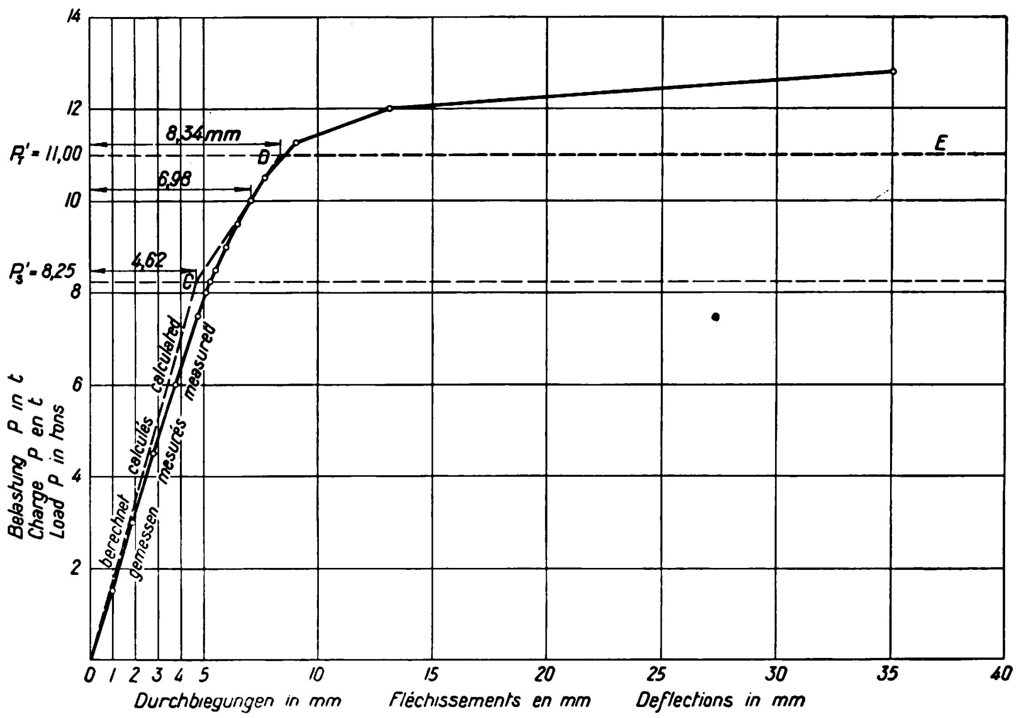

Fig. 8.

Case II.

The most important readings taken from this experiment are shown in Fig. 7. The mean deflection values are plotted on Fig. 8, while Fig. 9 shows the elonga-

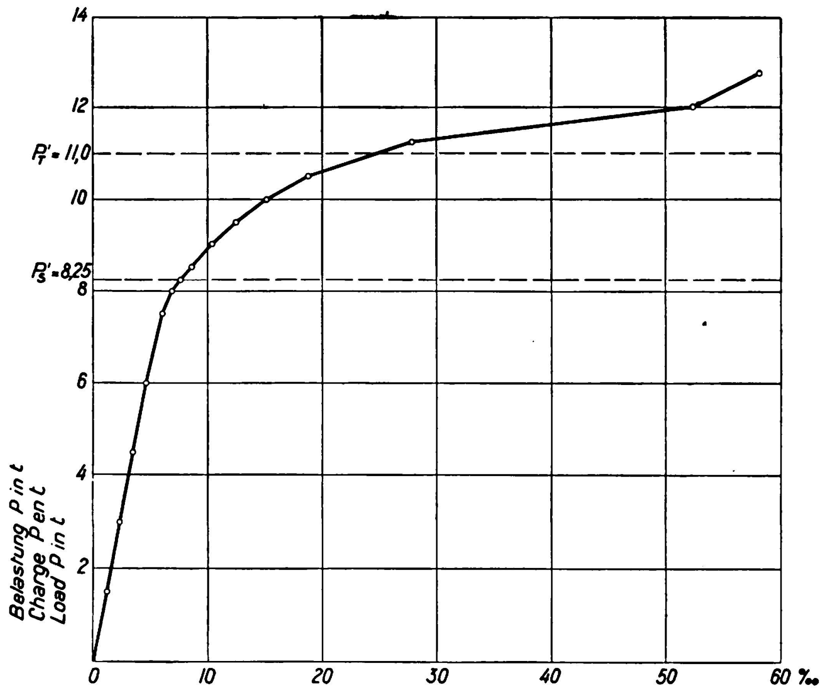

Fig. 9.

tions of a measured stretch of 100 mm on the upper flange over the central support. The properties of the compound beams based on actual measurements are: Sectional area $F = 43\ cm^2$; Moment of inertia $J = 1727\ cm^4$; Modulus of section $W = 211\ cm^3$ and an average yield stress of $2.51\ t/cm^2$ was found by tensile tests. If this latter value could be employed for calculating M'_s using the same notations as in section A, this bending moment would be $M_s = 211 \cdot 2.51 = \sim 530$ cmt. According to *M. Grüning* [2], M'_s would be $232 \cdot 2.51 = 585$ cmt

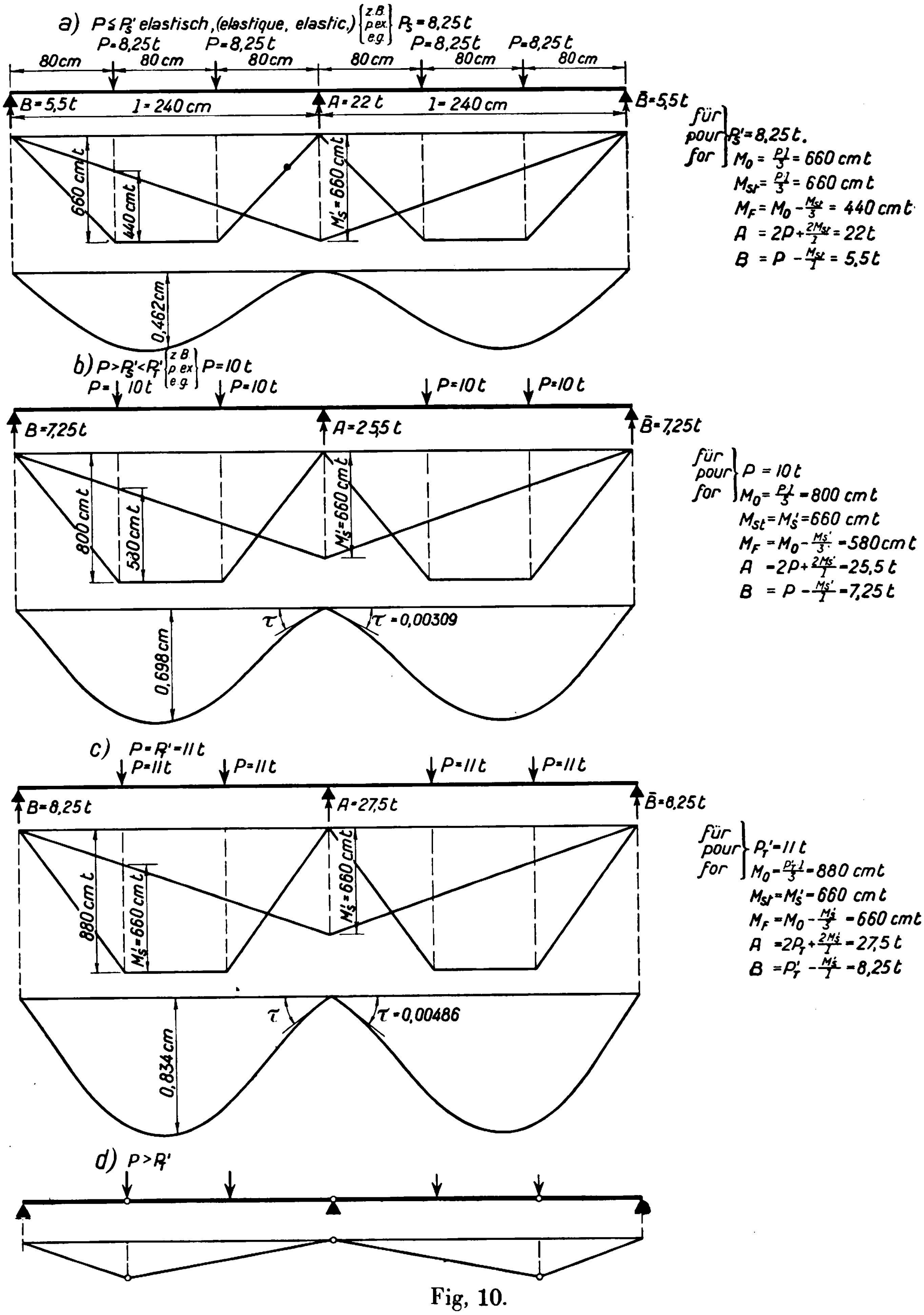

Fig, 10.

and according to *Fritsche* [3] p. 854, it would be $1.16 \cdot 530 = 620$ cmt. During the execution of the test the first traces of yielding were observed at the junction from web to the upper flange over the central support, for one joist under a load of P = 8.25 t (and for the other under a load of P = 8.50 t). The corresponding moment for this condition is $M'_s = \frac{P\,l}{3} = 8.25 \cdot 80 = 660$ cmt and $8.50 \cdot 80 = 680$ cmt respectively. It can be seen clearly from Fig. 8 that from $P'_s = \sim 8.25$ t onwards the deflections start to increase more.

To interpret this experiment by the simplified hypothesis given at the end of section A, th evalue $M'_s = 660$ cmt is used, and the results are shown on Fig. 10.

The quantity P'_s represents the value of P — assuming fully elastic conditions — for which the moment M_{st} over the support is equal to M'_s (Fig. 10a). This relation yields

$P'_s = \frac{M'_s \cdot 3}{l} = \frac{660 \cdot 3}{240} = 8.25$ t. If P should assume higher values than P'_s, the moments over the support will not increase above the value of M'_s (Fig. 10b). The carrying capacity is reached if a load P'_T produces under the point of attack of the outer load a moment $M_F = \frac{P'_T \cdot l}{3} - \frac{M'_s}{3}$ equal to M'_s, (Fig. 10c). Hence $P'_T = \frac{4\,M'_s \cdot 3}{3 \cdot l} = \frac{4 \cdot 660}{240} = 11$ t. From Fig. 8 can be seen, that indeed the deflections grow more rapidly with increasing loads above P = 11,25 t, thus rendering the beam useless for practical purposes. (If, as previously mentioned, the calculation had been based on $M'_s = 680$ cmt, we should have received $P'_s = 8.5$ t and $P'_T = 11.66$ t, which values correspond still better with the actual conditions).

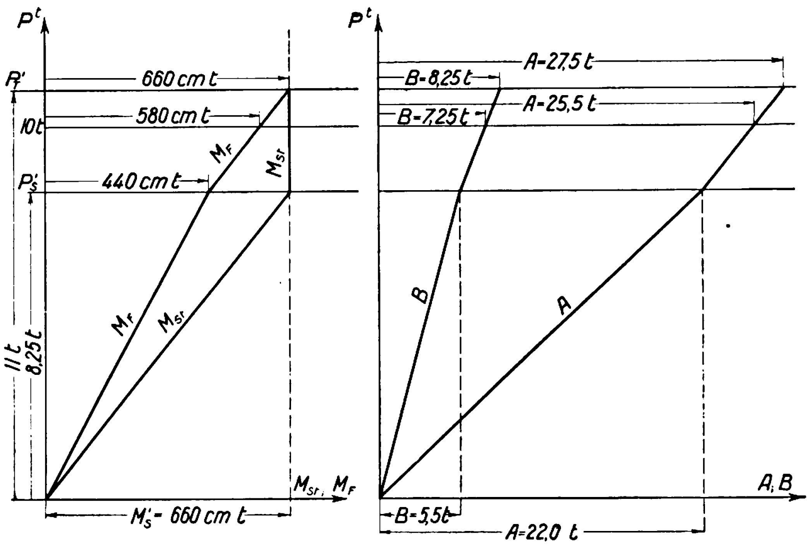

Fig. 11.

The values given in connection with Fig. 10 are plotted in Fig. 11.

In Fig. 10 and 12 are shown diagrammatically the deformations based on the simplified interpreting hypothesis with J = 1727 cm⁴, E = 2100 t/cm² but without considering the influence of shear. The deflections for the middle of the span 4.62 mm, 6.98 mm and 8.34 mm calculated with P = 8.25 t, P = 10 t and P = 11 t are shown in Fig. 8. To the basis of calculation corresponds the line OCDE of the deflections and further, that the deflections grow unrestrictedly when the value P'_T is reached.

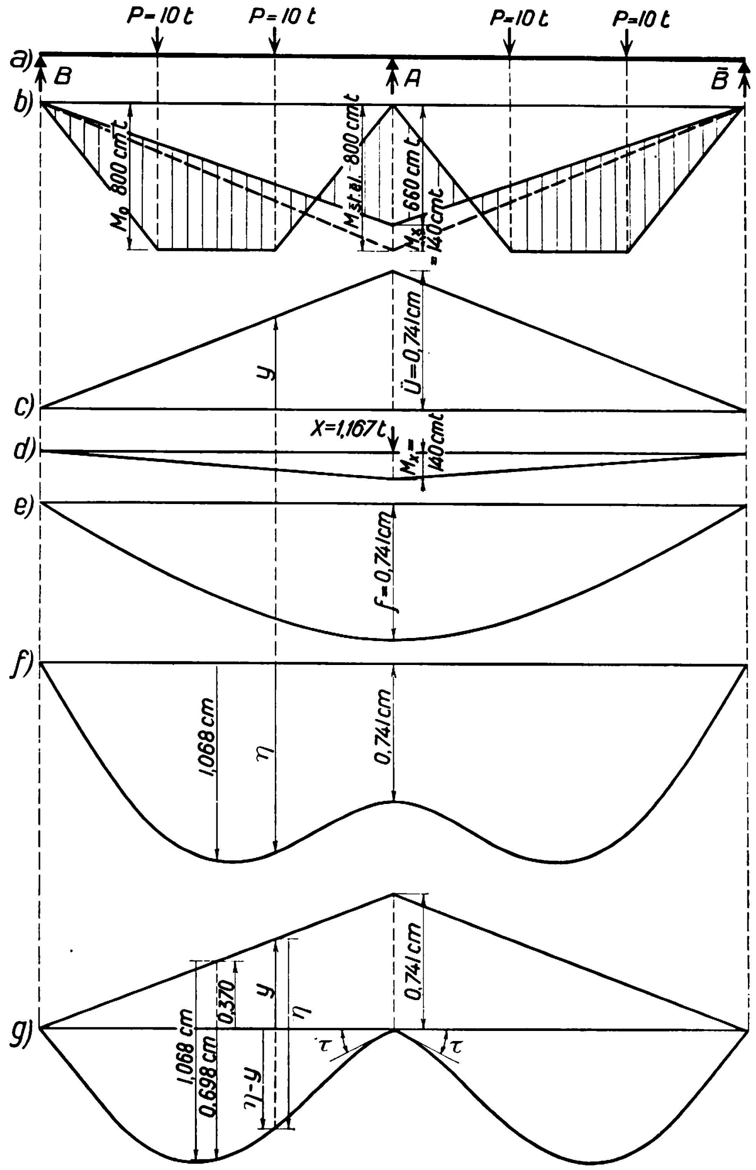

Fig. 12.

The simplified hypothesis makes it quite clear how in the range $P > P'_s < P'_T$ the equalization between the bending moment M_{st} over the middle support and the moment M_F in span takes place. The deflection line of the beam $B A \bar{B}$ (Fig. 10b) shows that at the point A which might be considered as a hinge, there is an abrupt change of direction of $\varphi = 2 \cdot 0.00309$. If the beam $B A \bar{B}$ is released from its load, it will assume the shape indicated by Fig. 12c with a camber ü = 0.00309 · 240 = 0.741 cm. On reloading the beam the camber ü must first disappear by a load $x = \frac{48\,E\,J\,ü}{l} = 1.167$ t

(Fig. 12e). This load corresponds to a positive bending moment at the support of $M_x = \frac{1.167 \cdot 480}{4} = 140$ cmt. When the beam now is loaded again with 10 t there is a total bending moment at the support of $M_{st\cdot el} - M_x = \frac{10 \cdot 240}{3}$ $- 140 = 660$ cmt (Fig. 12b). Since it is assumed that up to this bending moment of 660 cmt the strains are elastic, reloading with loads up to 10 t takes place within the elastic range. Finally the hatched area of the bending moment diagram given in Fig. 12b again appears. The whole procedure can also be
diagram given in Fig. 12b again appears. The whole procedure can also be
expressed in the following manner: If the beam is restrained from lifting from the support, firstly a restraining force X is acting and the corresponding moment $M_x = 140$ cmt. Due to the loads of 10 t the bending moment over the support now continues to increase quite elastically up to the value

$$M_{st\cdot el} - M_x = \frac{Pl}{3} - 140 = 10 \cdot 80 - 140 = 660 \text{ cmt.}$$

The deflections η of the reloaded beam B A $\overline{B}$ with the initial camber ü are received in the form of ordinates of a bending moment diagram for a beam B$\overline{B}$, loaded by $\frac{1}{EJ}$ — times the values of the hatched moment area given in Fig. 12b. (Mohr's method applied to cambered beam.) The deflection line, computed this way, is shown in Fig. 12f. The deflection a point A must check with camber ü. If the ordinates of the deflection curve η are plotted from the axis line of the cambered beam as a base (ordinates y) the shape of the axis of the reloaded beam is obtained. (Ordinates η — y.) This shape (Fig. 12g) is identical with the sape of the axis after the first loading with 10 t (Fig. 10b).

Comparing the preceding qualitative interpretation of the loading, unloading and reloading due to loads $P = 10$ t with the results received by experiments (Fig. 7) we find general agreement in two points. Firstly, after loading and reloading with 10 t a camber ü appears over the middle support and secondly, the reloading is perfectly elastic. Full numerical agreement cannot be expected for the following reasons:

a) the simplifying assumptions of the interpreting hypothesis,
b) differences in the geometrical properties of the beams,
c) differences in the behaviour of the beams under load (influence of shear on the strain, variations in modulus E and yield point stress σ_s),
d) the practical impossibility of keeping the supports exactly at the same level.

The experiments, however, show clearly that the moment over the support does not increase above the value of M'_s for loads above the value P'_s, although an increase of moments in the span takes place. The reason for this is that the beam automatically undergoes a deformation producing a camber ü as if established by cold bending in a machine. This phenomenon of producing a camber ü, reduces the bending moment over the middle support in exactly the same way as if the middle support were lowered artificially by the same amount. According to calculation we receive for $P = 10$ t and $P = 11$ t the values ü = 7.41 mm and 11.65 mm respectively. They are quite small for a beam of 480 cm in length. The values obtained by experiment are smaller.

The summary of this would be:

1) The interpretation and their simplified assumptions give a sufficiently accurate basis to judge the carrying capacity of the continuous beam under consideration. It is quite safe to introduce for a simply supported beam the carrying moment $M_s = W \cdot \sigma_s$ and to calculate with this moment according to Fig. 11 the values of P_s and P_T for the continuous beam under consideration.

2) The following definitions correspond to the simplified hypothesis of interpretation:

a) P'_∞ represents an ultimate load for which loading, unloading and reloading of the beam still produce only fully elastic deformations.

b) It is essential for $P > P'_s$ but less in value than the maximum load P'_T, that only limited and practically harmless deformations similar to cold bending of the beam are produced near the cross section where, according to the theory of elasticity, the maximum bending moment occurs. The unloading and recharging of the beam creates fully elastic deformations only.

c) P'_T represents an ultimate load for which, if exceeded, the beam enters into a condition of instability. (See Fig. 10d.)

3) The actual behaviour of the continuous beam is as follows:

a) P_s creates the first permanent although small deformations.

b) The deformations increase considerably with $P > P'_s$, though without impairing the practical usefulness of the beam.

c) For $P > P'_s < P'_T$ unloading and recharging of the beam takes place under fully elastic conditions.

d) With $P > P'_T$ the deformations grow to such an extent as to render the beam useless for practical purposes.

e) At P_v the beam fails completely.

The interpretation of the test results of cases III and IV need not be gone into here. In comparison with case II, the load P'_s entered later into account for case III, and earlier for case IV, but P'_T was found to have almost the same value in all three cases.

An article published in [12] describes tests proposed by *J. H. Schaim,* with simply supported single span and continuous double span beams, spanning 4 m, and loaded with four equal point loads in each span. (See Fig. 13 and also [13].)

It can be assumed that $M'_s = \sim 614$ cmt ($= \sim 234 \cdot \sigma_s = 234 \,.\, 2.62$) as for test I for a simply supported beam loaded with four equal point loads P, with $\sigma_s = 2.645$ t/cm², the beam failed at $P_v = \frac{10}{4}$ t corresponding to a bending moment of $240 \cdot \frac{10}{4} = 600$ cmt. For test 4 with $\sigma_s = 2.895$ t/cm² the deformations grow rapidly for a load of $P = \frac{10}{4}$ t. The load P_v of this simply supported beam was found to be $\frac{12.03}{4} = 3.01$ t.

For the above mentioned value $M'_s = 614$ cmt the load P'_s assumes the value

$P'_s = \frac{614}{240} = 2.56$ t. It can be seen from Fig. 13c (total and elastic elongations in span and over support) that permanent deformations developed already at $P = 2$ t. The probable explanation for this is that as stated [12], p. 14 'a relative lifting-off of the middle support has taken place, thus causing increased stressing over the intermediate support'. Therefore M_{st} become equal to M'_s

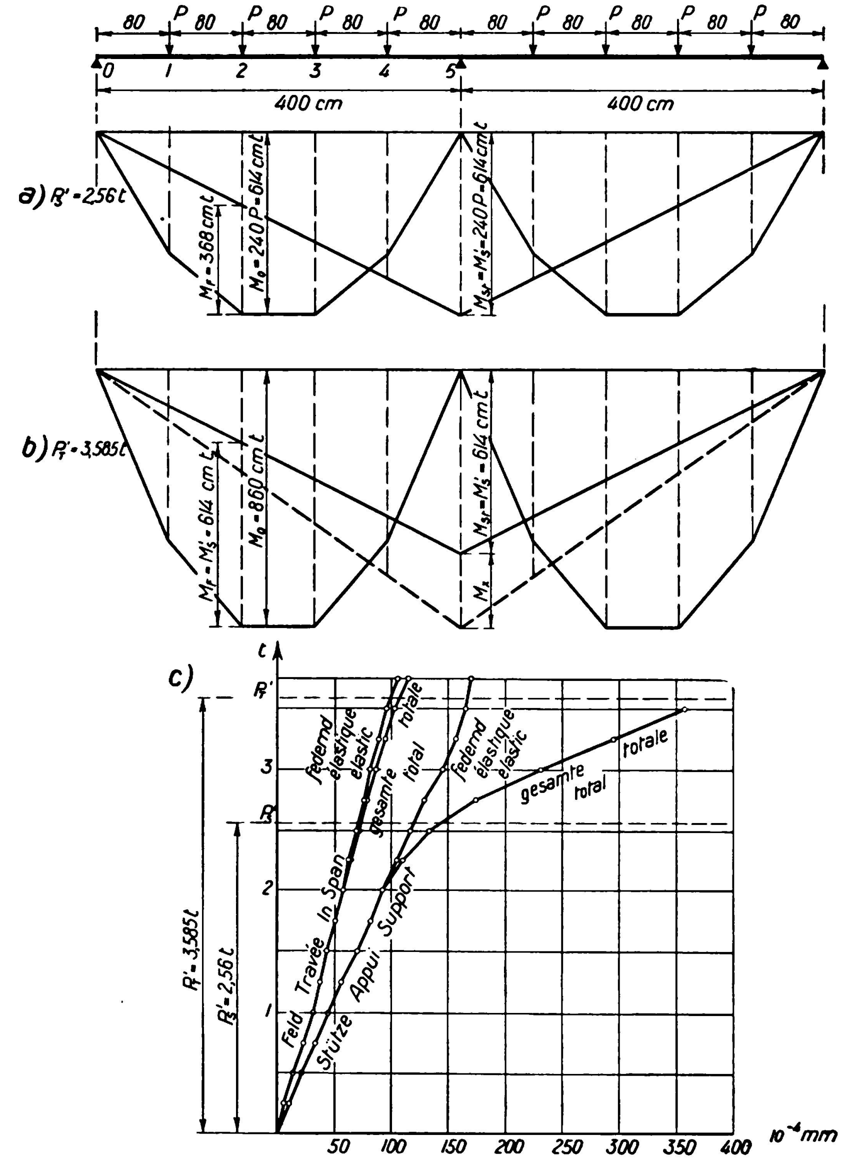

Fig. 13.

even at $P < P'_s$. The load P'_T is reached since for the cross section 2 the moment $M_F = M_O - \frac{2}{5} \cdot M_{st} = M'_s$, i. e. $240\,P'_T - \frac{2}{5}\,M'_s = M'_s$, hence $P'_T = 3.585$ t. The beam fails at $P_V = \frac{19}{4} = 4.75$ t.

The foregoing and the following remarks are concerned with loads increasing from o to P'_T (to P_V) whilst the tests of *O. Graf*, published in [14], deal with the investigation of the fatigue strength of simply supported single span and continuous double span beams of steel St. 37.

C. Continuous I-beams over two spans, with only one span loaded.

If a continuous beam (Fig. 14) having two equal spans AB and BC is loaded with a point load P at the distance a from the left outer bearing, all deformations remain fully elastic until P reaches the value P'_s or in other words as long as the moment M_F in the span remains smaller than M'_s. The closing line

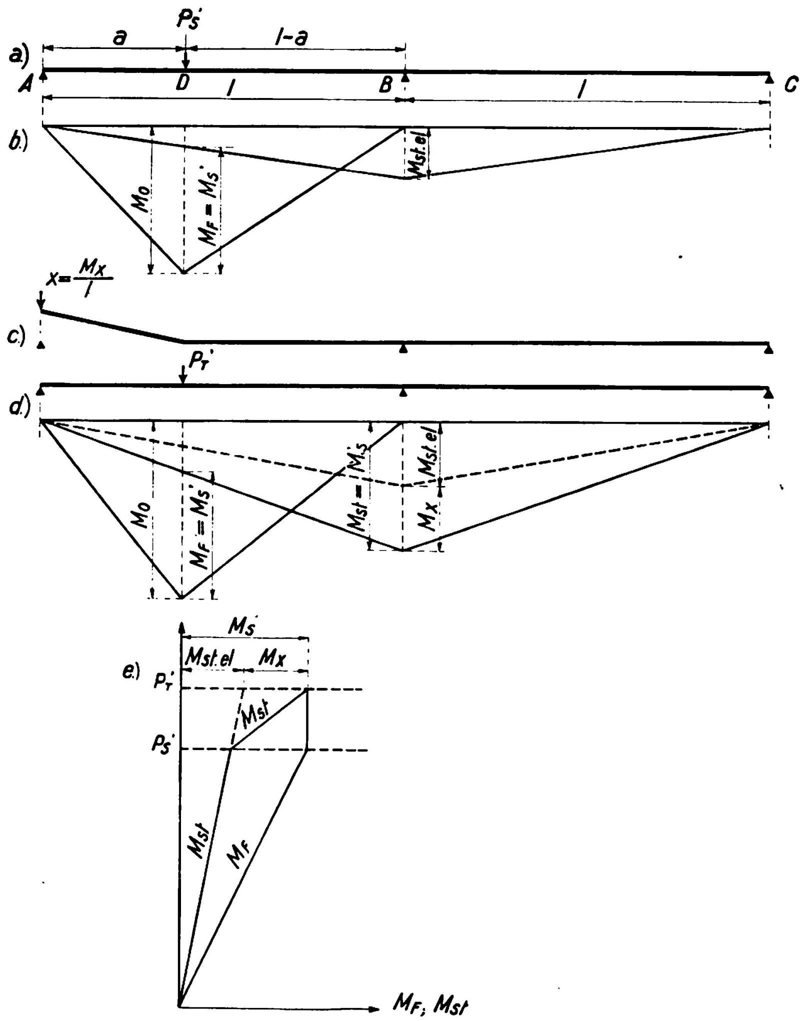

Fig. 14.

of the bending moment diagram (Fig. 14b) is determined by $M_{st\ el}$. For loads $P > P'_s$ the bending moment diagram corresponds to the M_O-diagram and a closing line determined by the stipulation that the moment M_F in the span shall not exceed M'_s. The ultimate value of the load P'_T is attained at $M_{st} = M'_s$ (Fig. 14d) according to the following condition:

$$\frac{l - a}{l} \cdot a \cdot P'_T - \frac{a}{l} \cdot M'_s = M'_s$$

hence

$$P'_T = \frac{M'_s \left(1 + \frac{a}{l}\right) l}{a\,(l - a)}$$

The relations M_F (P) and M_{st} (P) are shown in Fig. 14e.

For $P > P'_s < P'_T$ and for $P = P'_T$ (Fig. 14d) and in accordance with the explanations given in section B, the moment M_{st} over the central support can be considered as composed of two parts: $M_{st \cdot el}$ and $M_x = M_{st} - M_{st \cdot el}$. A visible lift away from the support (cold bending at the attack of the load) (Fig. 14c) corresponds to the bending moment M_x in such a way that on reloading with the force $X = \frac{M_x}{l}$ the end of the beam can be brought back again to the support. Afterwards, for loads increasing from o to P all deformations are again fully elastic, and the elastic bending moment $M_{st \cdot el}$ produced by P has to be added to the moment M_x due to X. The shape of the bent beam (Fig. 14c) could also be derived from the deflection line of the span AB, similarly as shown in section B the test carried out by F. Hartmann and described in [4] is based on a beam charged with two point loads in the left span. The beam used was an I-beam with a depth of 12 cm with the following properties: $J = 328\ cm^4$; $W = 54.7\ cm^3$; $\sigma_s = 2.51\ t/cm^2$; $M_s = 54.7 \cdot 2.51 = 137.5$ cmt. If we choose $M'_s = 160.9$ cmt $(= \sim 1.16 \cdot M_s)$, according to data given in [4] p. 79, we receive following the simplified hypothesis of interpretation the conditions shown in Fig. 15 and 16. As long as $P < P'_{s1}$ the distribution of

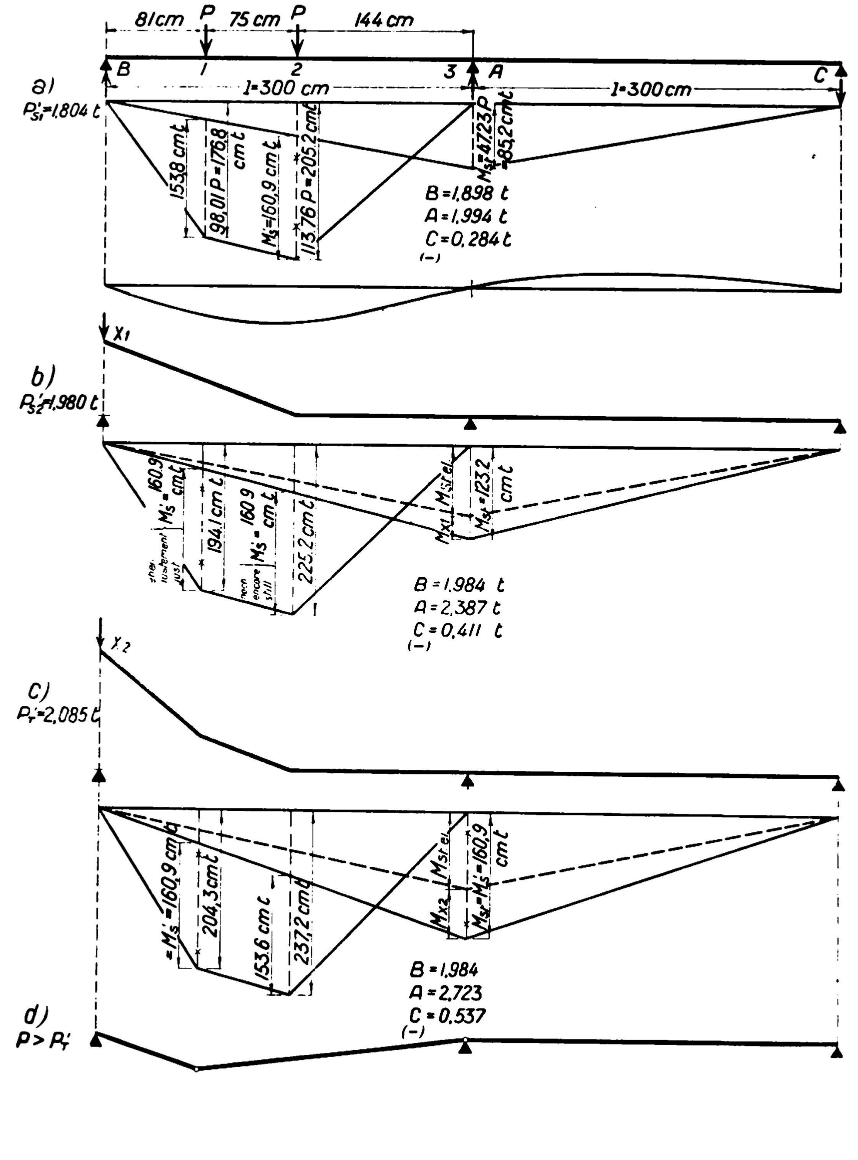

Fig. 15.

moments is established by the M_O — diagram and the closing line, fixed by the moment $M_{st\ el}$. The moment in the cross section 2 of the beam (Fig. 15a) attains M'_s for a load $P'_{s1} = 1.804$ t. For the loads $P = P'_{s1}$ and subsequent unloading the beam undergoes permanent bending in point 2 (cold bending). The same values M'_s are obtained for the bending moments in point 1 and 2 if $P = P'_{s2} = 1.98$ t (Fig. 15b); but for $P > P'_{s2}$ the bending moment under point 2 is less than M'_s. If the beam is released of its loads we observe a further bending-up of the beam at point 1. The moment at point 1 and the moment over the support become equal to M'_s for an ultimate load $P'_T = 2.085$ t (Fig. 15c). The moment over the support e. g. of Fig. 15c can again be considered as consisting of two parts: M_{x2} and $M_{st \cdot el}$, as previously explained. To the part-moment M_{x2} belongs a force X_2 which for recharging of the beam causes the previous permanent deformation to disappear at the support A, allowing in consequence the beam to undergo fully elastic deformations again. The relations between M_1, M_2, M_{st} and P are shown diagrammatically in Fig. 16; in addition to this are shown the strain values ε_1, ε_2 and ε_3 received by experiment from various stages of loading taken from [4] (Fig. 13). It can be seen that the elongations ε_2 are greater than ε_1 provided the bending moment at point 1 has not reached the value M'_s. For $P = 1.94$ t, a value close to $P'_{s2} = 1.98$ t, the two lines cross each other, i. e. for $P > 1.94$ t the elongations ε_1 are greater than the elongations ε_2. The test was stopped at $P = 2.2$ t.

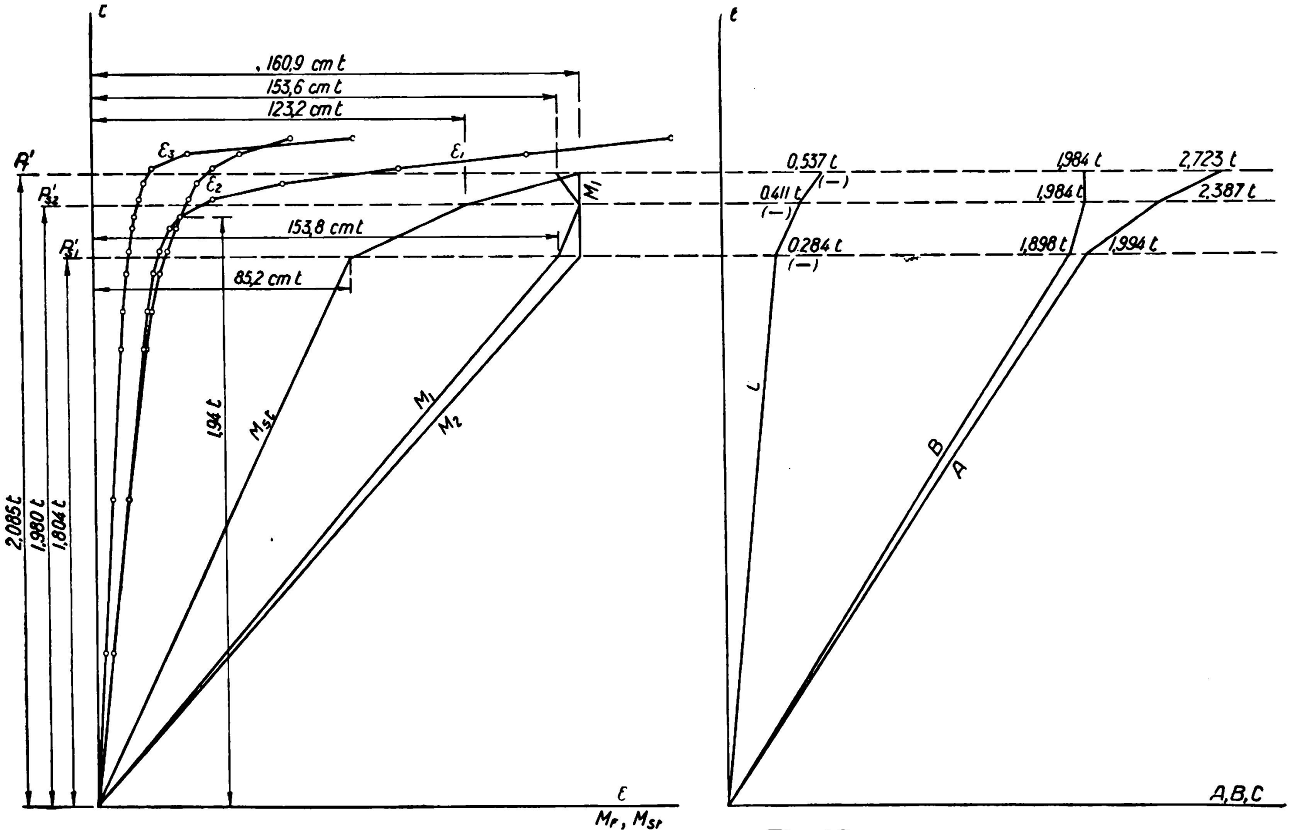

Fig. 16.

D. I-beams fixed at both ends.

a) Tests carried out in such a manner, that the cross sections at the supports remain vertical.

From the tests carried out by the Author and publshed in [1] only the tests for beam No. 11 shall receive consideration in the following.

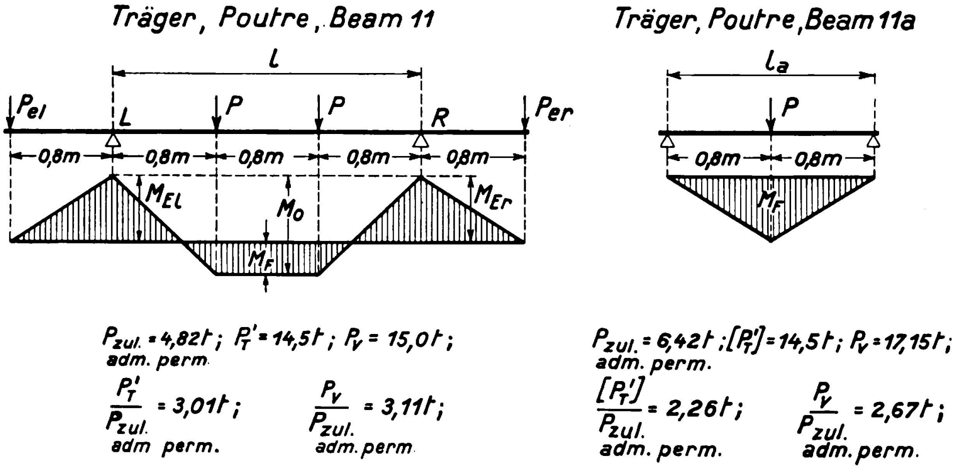

Fig. 17.

In Fig. 17 are shown side by side as previously in Fig. 5 of section B the values of P_{zul}, P'_T and P_V for a fixed beam (beam 11) and a simply supported beam (beam 11a); the behaviour of this simply supported beam has already been explained in section A. Both beams No. 11 and 11a were cut from the same I-beam 40 cm · 40 cm. The forces P_e shown in Fig. 17 were determined during the test and act in such a way as to keep, for all ranges of loading the cross sections of the beam at L and R perfectly and permanently vertical, with the purpose of establishing as nearly as possible the proper conditions required for the calculation of beams with fixed ends.

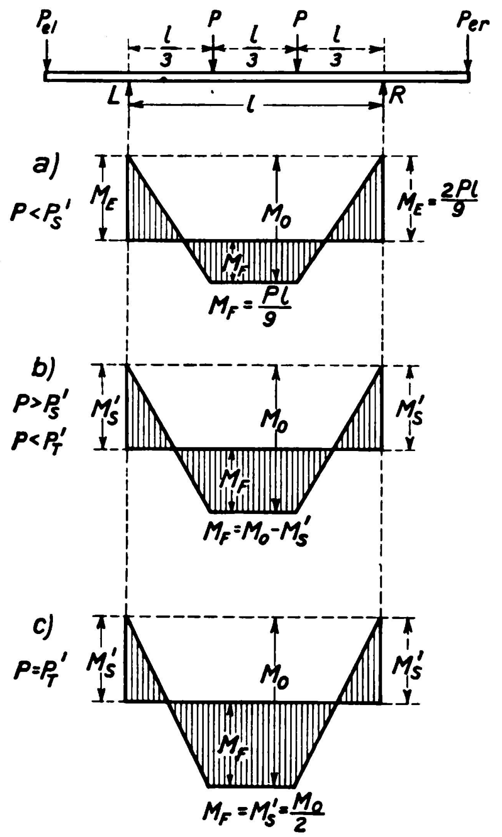

Fig. 18.

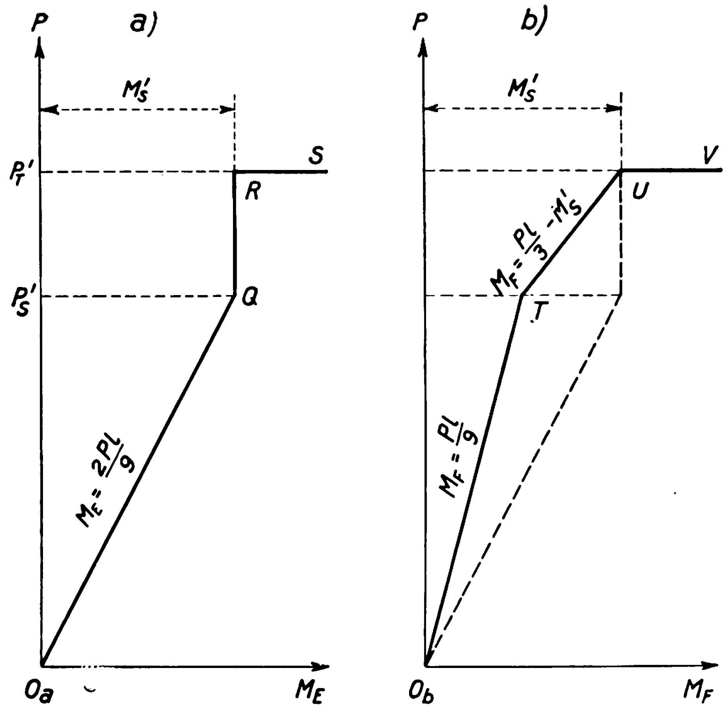

Fig. 19.

In accordance with the explanations given in the sections B and C and with the simplified hypothesis of interpretation the following various stages of loading of a beam with fixed ends are shown in Fig. 18:

a) For a load $P < P'_s$ (Fig. 18a) all deformations are of an elastic nature. Accordingly we receive:

$$M_O = \frac{P\,l}{3}, \quad M_E = \frac{2\,P\,l}{9}, \quad M_F = M_O - M_E = \frac{P\,l}{9}.$$

b) Due to a load $P'_s = \frac{9 \cdot M'_s}{2\,l}$ the moment over the support reaches the value of the carrying moment M'_s. For $P > P'_s$ the moments M_E cannot go much beyond the value of M'_s (Fig. 18b). The following relations apply:

$$M_E = M'_s; \qquad M_F = M_O - M'_s.$$

At this stage a change of the angle between the tangent of the deflection curve and the previously horizontal axis of the beam takes place. For elastic deformations only this tangent is horizontal. After the beam is released from its loads, a permanent deformation (cold bending) is observed in such a way that the ends of the beam at the left of L and at the right of R point downwards. To fulfil the assumptions on which the calculations of the beam with fixed ends are based it is necessary, before recharging of the beam takes place, to apply forces P_{el} and P_{er} (each equal to X, Fig. 20b), acting upwards, bringing the cross section of the beam at L and R into vertical position again. The moments M_s produced by this action, can be found in a similar way as explained under B and C:

$$M_x = M_{E \cdot el} - M'_s.$$

c) Due to P'_T the moment at the place of attack becomes $= M'_s$, i. e. it is expressed by the following term:

$$M_F = \frac{P'_T \cdot l}{3} - M'_s = M'_s; \text{ hence } P'_T = \frac{6\,M'_s}{l}.$$

Should the loads still increase, above the value of P'_T, then the beam enters into a state of instability.

The relations M_E (P), M_F (P) are plotted in Fig. 19, from which diagram the values for P'_s and P'_T for a given value of M'_s can readily be taken.

The simply supported reference beam 11a of Fig. 17 treated in section A furnishes the following relation:

$$M'_s = \frac{[P'_T] \cdot l_a}{4} = \frac{14.5 \cdot 160}{4} = 580 \text{ cmt.}$$

Accordingly we receive from the formula given above under b):

$$P'_s = \frac{9.580}{2.240} = 10.87 \text{ t},$$

and from the formula laid down under c):

$$P'_T = \frac{6 \cdot 580}{240} = 14.50 \text{ t}.$$

Under observance of the simplified mode of calculation of the sections A and B and with $J = 1525\ cm^2$, $E = 2100\ t/cm^2$, the deformations due to the ultimate loads $P'_s = 10.87$ t and $P'_T = 14.5$ t respectively, are shown in Fig. 20, in combination with the relations $f(P)$ and $\tau(P)$.

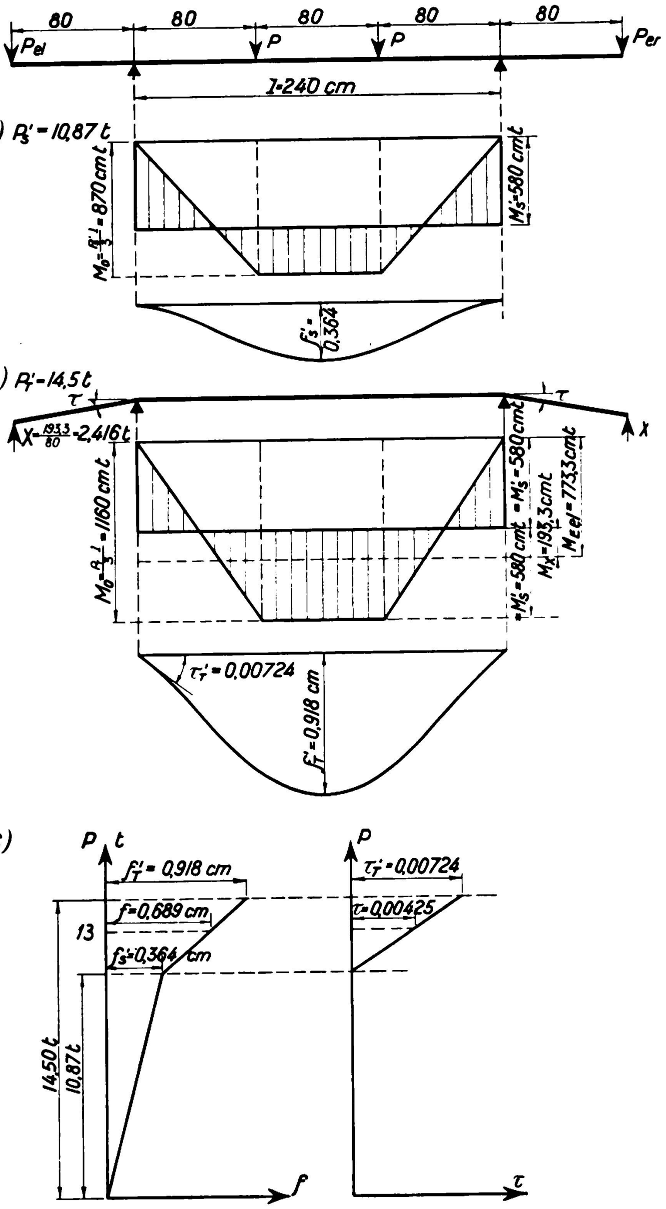

Fig. 20.

As mentioned, during the execution of the tests the auxiliary forces P_{el} and P_{er} were measured and in consequence also the restrained moments M_E || $80 \cdot P_e$ together with the moments $M_F = M_O - M_E$. These values, in analogy to Fig. 19, were entered in Fig. 21. This Fig. shows also the lines OQRS and OTUV for M_E and M_F, according to the values of P_s and P_T, calculated by means of the relation $M_s = W\,\sigma_s$. This procedure may be recommended if it is desired to be on the safe side when preparing the analytical calculation for the actual carrying capacity of a beam. For the purpose of comparison the values f of deflections measured in mid-span are shown in Fig. 22, while Fig. 20 illustrates the corresponding calculated quantities. The measured values become higher for $P < P_s$ compared with the calculated deflections. The reason for this may be, as shown in Fig. 21, that the actual bending moments in the span produced by the test are higher than the calculated values.

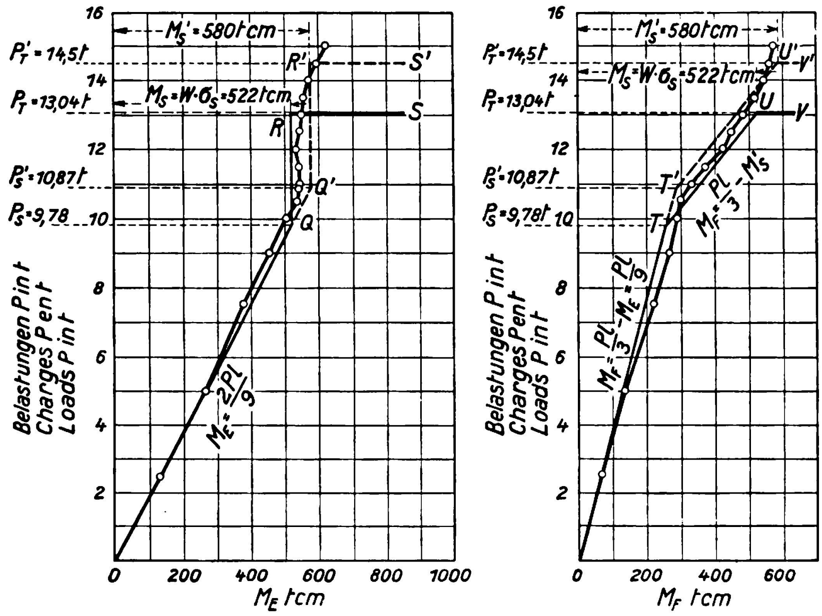

Fig, 21.

Beam 11.

Of particular interest are the permanent deflections of the beam ends shown in Fig. 23. The deflections are proportional to the angles τ (Fig. 20) if the assumptions made for calculation are observed. Fig. 24 gives the measured unit tensile elongations at the supports and in mid-span.

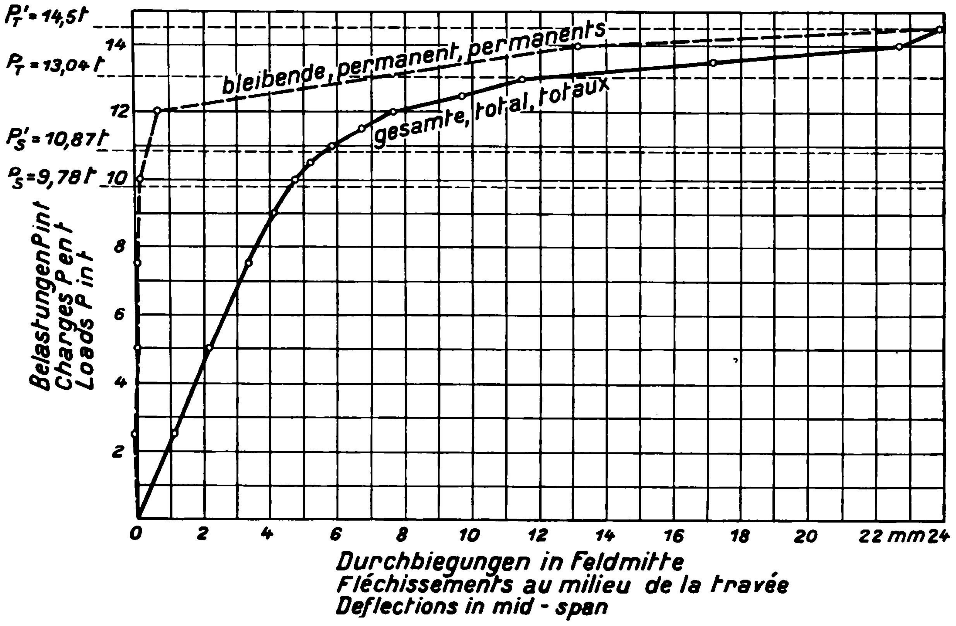

Fig. 22

d) Test with I-beams, ends fixed in masonry.

G. v. Kazinczy published in [15] tests which he carried out with I-beams with a depth of 160 mm, having clear spans of 5.60 and 6.00 m[4]. The size

[4] The Author heard of the first mentioned tests at the end of 1928 and of the second tests only in 1930.

of the beams was based on a bending moment of $M = \frac{p\,l^2}{24}$. The deficient carrying capacity at the supports was supplied by providing top reinforcement of round bars and a concrete slab acting as compression flange. Based on

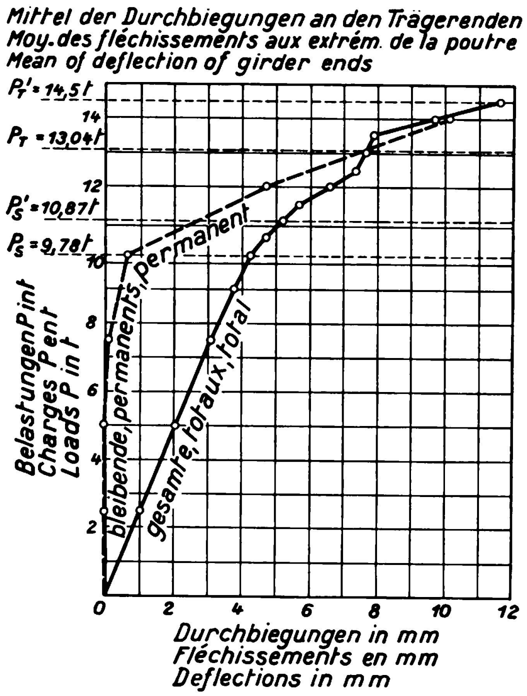

Fig. 23.

these tests, *G. v. Kazinczy* proposed that a beam with fixed ends not encased in concrete should be designed for a moment of $\frac{p\,l^2}{16}$, irrespective whether the

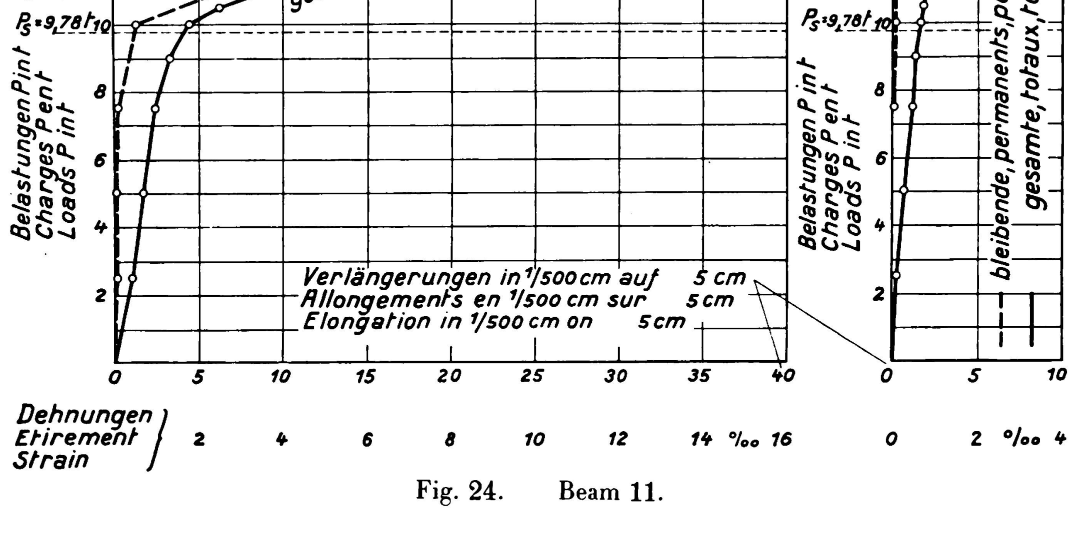

Fig. 24. Beam 11.

beam be fully or only partially fixed. He also points out that such cross sections having reached the yield point stresses may be regarded as acting like a hinge, equipped with a permanent bending moment.

F. v. Emperger reports in [16] on experiments carried out with one simply supported beam and six beams with ends fixed in different kinds of masonry. The beams used were I-beams No. 15 with a clear span of 4 m[4]. In his report

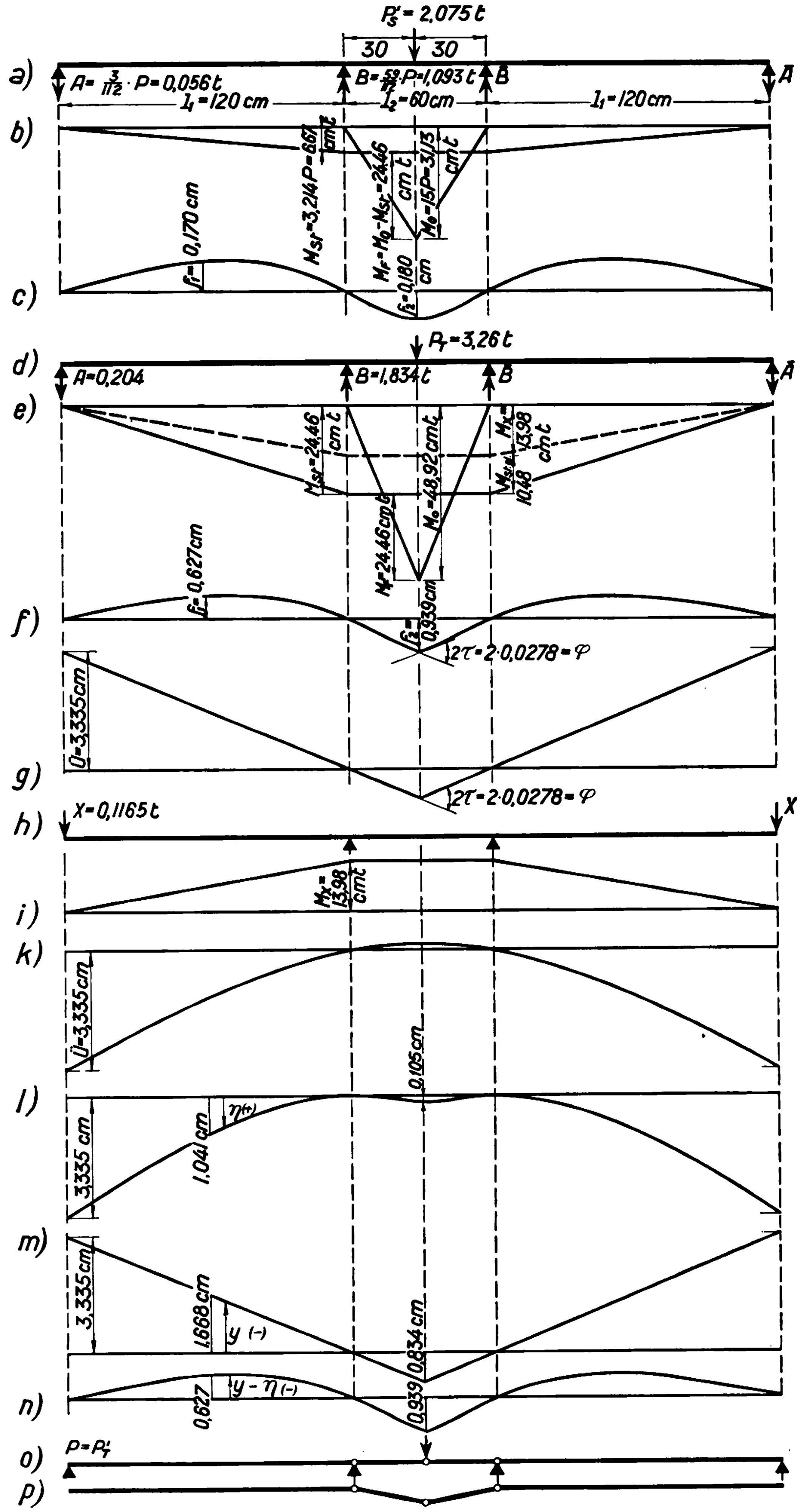

Fig. 25.

F. v. Emperger says 'that provided certain conditions for fixing in masonry are observed, the carrying capacity of steel beams can be expected to be such as almost to reach the attainable maximum bending moment of $\frac{Pl}{16}$.'

E. Continuous I-beams over three spans, with loaded central span.

Such beams were studied and tested by *F. Stüssi* and *C. F. Kollbrunner* as published in [6] (especially tests 532/6 and 534/8). The behaviour of a

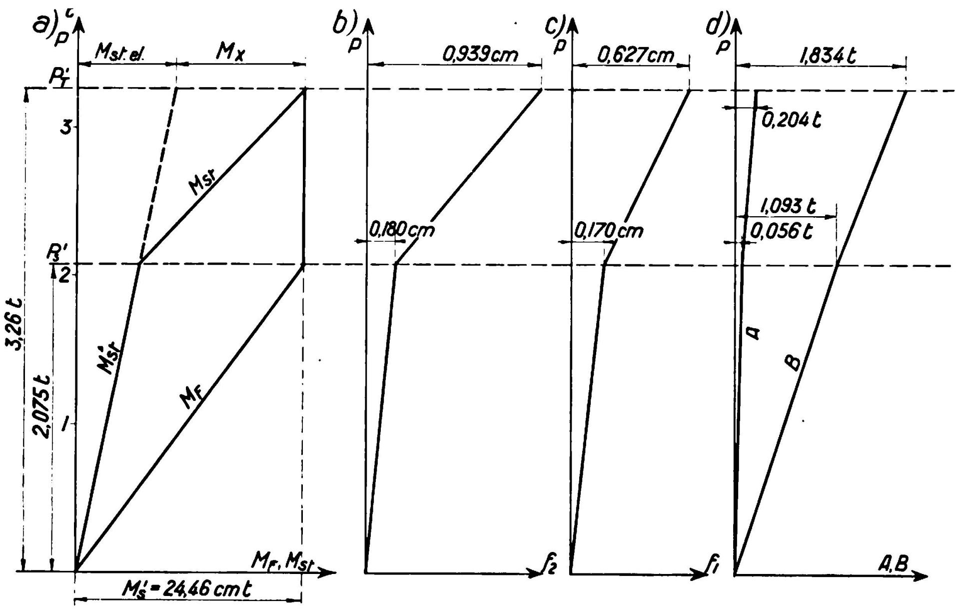

Fig. 26.

beam corresponding to these tests for loads ranging from o to P'_T under consideration of the simplified hypothesis of interpretation, is shown in Fig. 25 and 26. For the beam I $\frac{46}{35}$ is $J = 16.73$ cm^4 and $W = 7.28$ cm^3. Specimens cut from the flanges gave an average yield point stress of $\sigma_s = 3.36$ t/cm^2 with margins of $\pm 10\%$. The results of the tests 532/6 and 534/8 (see Fig. 14 and 15 [6] which are identical to Fig. 27 of this report) allow to

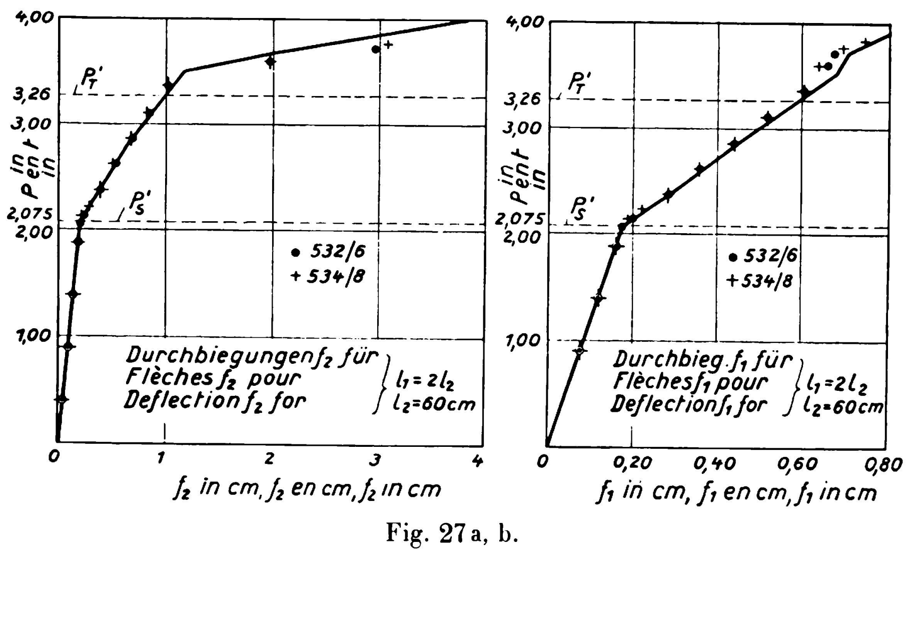

Fig. 27 a, b.

deduce that only incidentally $M'_s = 7.28 \cdot 3.36 = 24.46$ cmt.[5] This, since for the range of elastic deformations, under the sole consideration of deformations due to bending moments only, is

$M_{st} = 3.214$ P and $M_F = (15-3.214)$ P $= 11.786$ P, hence we receive $P'_s = \frac{24.46}{11.786} = 2.075$ t. According to Fig. 26a and for $P > P'_s$ the bending moment over the support is equal to $M_O - M_F = 15\,P - M'_s$; therefore with $15\,P'_T - M'_s = M'_s$ we receive $P'_T = \frac{2 \cdot 24.46}{15} = 3.26$ t. In agreement with the procedure adopted under A), B) and C), Fig. 25b shows the deflection curve for the ultimate load $P'_s = 2.075$ t under consideration of $E = 2100$ t/cm² and deformations due to bending moments only. In the bending moment diagram of Fig. 25e produced by the ultimate load $P'_T = 3.26$ t is $M_O = 15\,P = 48.92$ cmt, and $M_{st} = 48.92 - 24.46 = 24.46$ cmt. For the conditions of Fig. 25e the deflection lines (shape of beam axis) passing from A to B and $\bar{A}$ to $\bar{B}$ are designed in Fig. 25f. At the centre of l_2 an angle of $\varphi = 2\,\tau = 2 \cdot 0.0278$ can be observed. After release the beam assumes the shape shown in Fig. 25g, with lifting up at A and $\bar{A}$ to the extent of $ü = 0.0278 \cdot 120 = 3.335$ cm. Whilst reloading the elevation ü has first to be brought back again by introducing the forces $X = 0.1165$ t, to which corresponds the bending moment diagram of Fig. 25i and the deflection curve of Fig. 25k showing deflections at A and $\bar{A}$ identical with $ü = 3.335$ cm. The reloading of the beam with $P'_T = 3.26$ t causes elastic deformations only. The same bending moment diagram as given by Fig. 25e is reproduced through the combination of $M_x = 0.1165 \cdot 120 = 13.98$ cmt and the moment over the support $M_{st\,.\,el} = 3.214 \cdot 3.26 = 10.48$ cmt. The reaction at A is composed of two parts: the force X and the force due to merely elastic action of the beam: $\frac{3}{112} \cdot 3.26 = 0.0873$ t, both together $= 0.204$ t. The deflection line (Fig. 25l ordinates η) of the beam deformed as in Fig. 25g was calculated, starting with the supports $B\bar{B}$, according to the bending moment diagram given by Fig. 25e. The shape of the axis of the beam after reloading with $P'_T = 3.26$ t (Fig. 25n) is found by forming algebraically the quantities $\eta + y$, giving for instance in mid-span of the central bay a deflection $f_2 = 0.105 + 0.834 = 0.939$ cm and in mid-span of the end spans a deflection $f_1 = 1.041 - 1.668 = -0.627$ cm.

In the same way as in the sections B) and C) and according to Fig. 25c and f the relations between P and 1) the deflection f_2 in the intermediate span, 2) the deflection f_1 in the outer span, 3) the reaction A, 4) the reaction B are shown in Fig. 26b to 26d.

For the purpose of comparison are given in 27a and b the measured de-

[5] According to a letter received from Mr. F. Stüssi, the curve of deflections for a simply supported reference beam of $l = 60$ cm loaded in mid-span gives us: $[P'_T] = 1.71$ t corresponding to $[P_T] = 1.63$ t. In place of $M'_s = 24.46$ cmt the value $M'_s = 1.71 \cdot 15 = 25.65$ cmt had possibly been introduced for the interpretation of the test. But with $M'_s = 24.46$ cmt one is safe in calculating the value P'_T.

flections; the values for P'_s and P'_T are also entered in the same figures. It can be seen quite clearly that the quantity P'_T actually defines the actual carrying capacity.

It is not advisable to call the test result $P_w = 3.902$ t the carrying capacity, this has been explained already in the sections A) and B). For $P > P'_T$ the deflections increase much quicker than for $P < P'_T$. The measure results of the deflections agree well enough with the results received by the calculation based on the simplified hypothesis of interpretation.

To study the flow of moments due to $P > P'_s < P'_T$ more closely, the Author carried out in May—June 1936, two tests (see [17]) with loading as in Fig. 25 using an I-beam 10 · 10 cm with spans of $l_1 = 2.40$ m and $l_2 = 1.20$ m.

From a comparison test carried out with a simply supported single span beam loaded in mid-span was found $M'_s = 262$ cmt. Under elimination of the dead weight and the deformation due to shear we get: $P'_s = 11.12$ t and $P'_T = 17.47$ t.

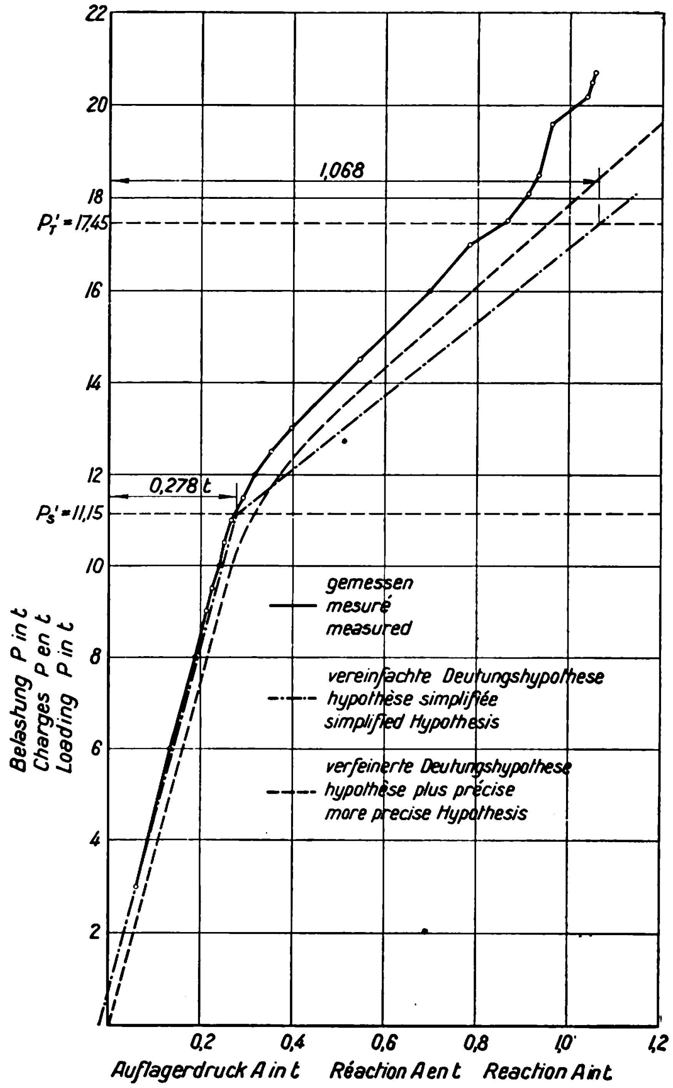

Fig. 28a.

In Fig. 28a are plotted the average values (received by test) for the reactions at A and $\overline{A}$, in Fig. 28b the bending moments M_F and M_{st}, calculated with the help of the measured values A and $\bar{A}$ under consideration of the dead weight. The influence of dead weight has also been considered in connection with $P'_s = 11.15$ t and $P'_T = 17.45$ t. The measured deflections in the centre of the intermediate span are given in Fig. 28 c.

The details of Fig. 28b show that the actual moments M_F and M_{st} deviate quite considerably from the values (shown in dash-dotted line) worked out

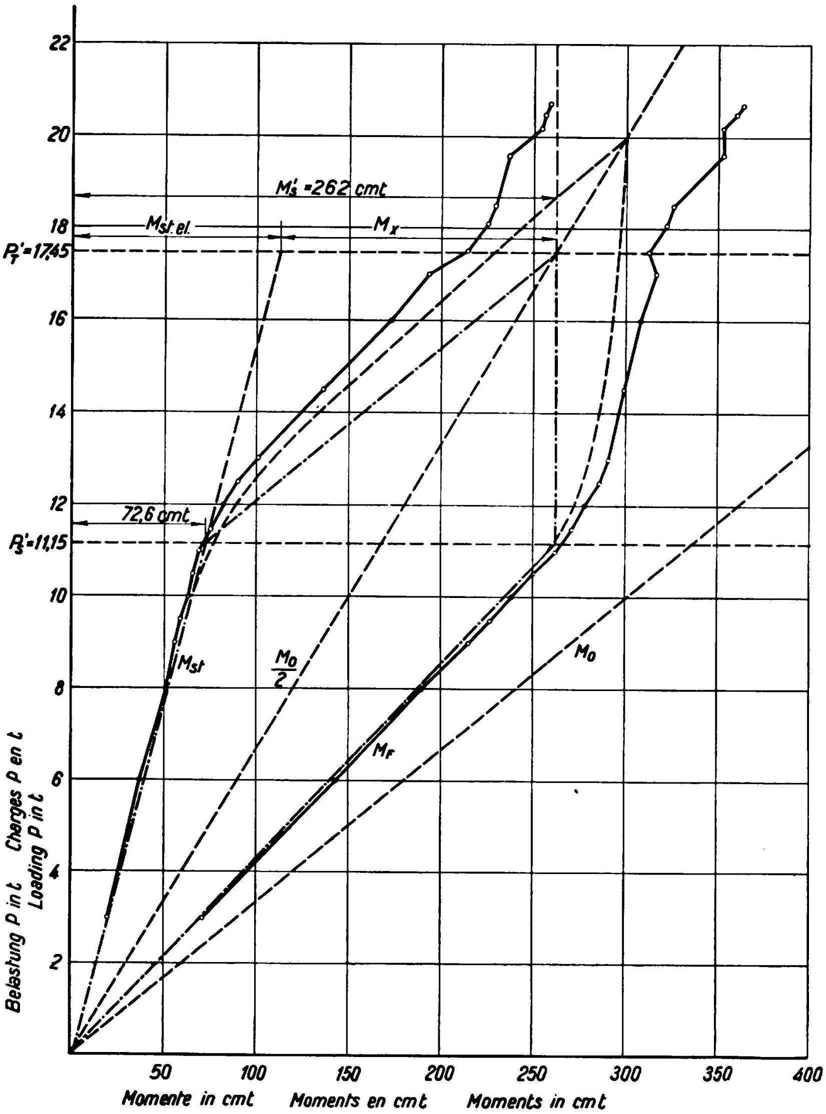

Fig. 28 b.
The dotted lines for M_F and M_{st} naturally hold only so long as $M_{st} < M_s$. The load P' corresponds to this limiting case. When this load is exceeded the beam buckles not only in the middle but also at the points of support.

according to the simplified hypothesis of interpretation. It is obvious that the quantities P'_s and P'_T are characteristic for the actual behaviour of the beam. (See also Fig. 28c, from which it will be noticed that the deflections f_2 increase only very considerably for values greater than P'_T.) The bending moments M_F exceed the value of M'_s if $P > P'_s$. The practical limit for the carrying capacity of the beam is only attained if permanent deformations develop also over the supports, or differently expressed, if M_{st} reaches the value of M'_s.

In any case, from the fact that both moments M_F and M_{st} are not equal for P'_T, it cannot be deduced that the practical limit of the carrying capacity of a continuous girder will be less than for P'_T. The deviations in the actual values of M_{st} and M_F can be explained by the choice of a straight horizontal line F G in Fig. 4 to replace the curve C D E, in accordance with the simplified hypothesis of interpretation. Based on the line CDE established by test results and under elimination of the influences of dead weight and deformation due to shear we find the bending moment M_F and M_{st} as shown dotted in Fig. 28 b in conformity with what we said in [17].

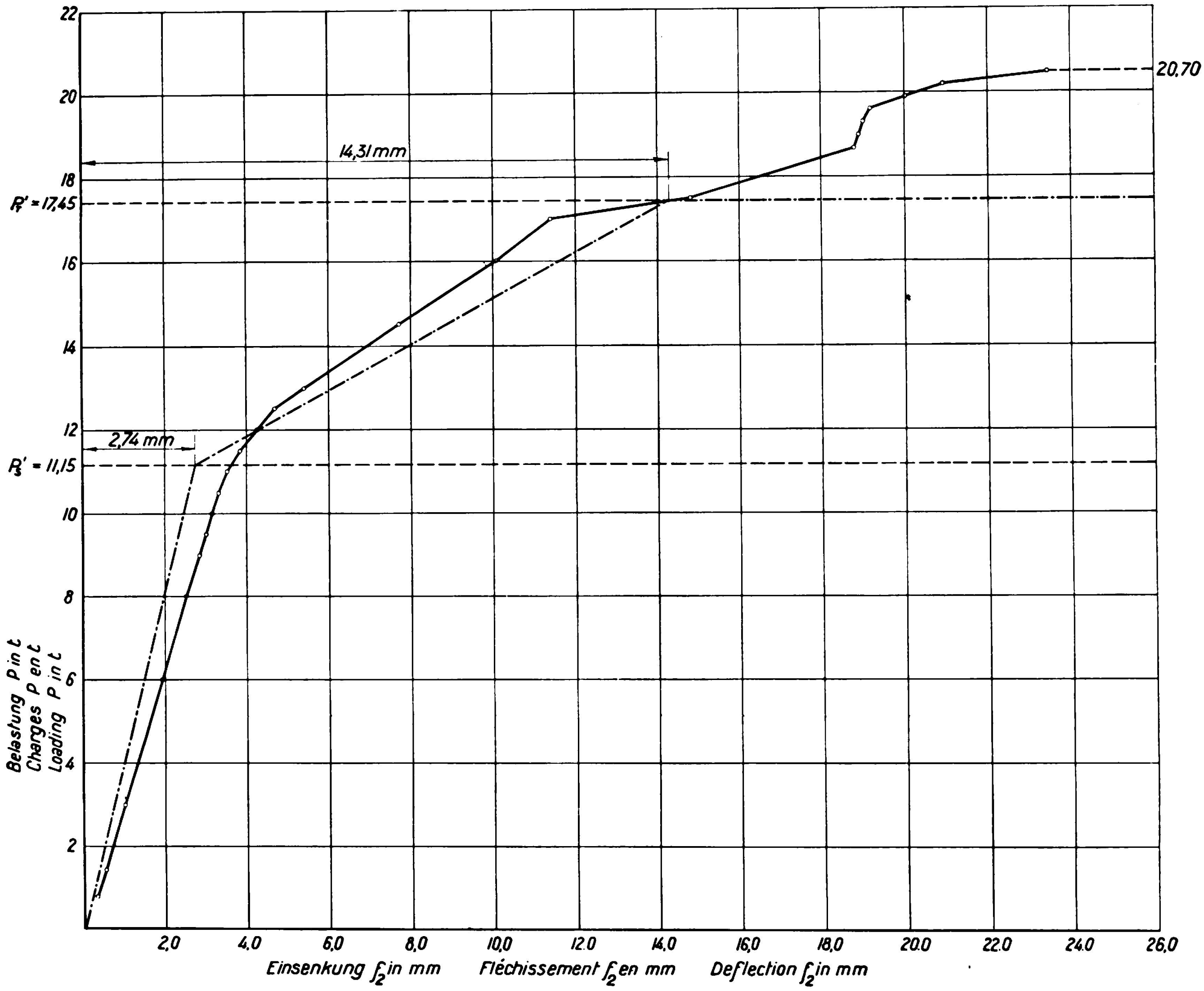

Fig. 28c.

F. Continuous latticed girders with parallel chords, over three spans.

The tests started by *M. Grüning* and completed by *G. Grüning* and *E. Kohl* were based on the type of girder shown in Fig. 29a (see [18]). The bars above the intermediate supports B $\overline{B}$ in the top chord and the three bars in the centre of the lower chord are removable I-bars. The panel point No. 17 was subsequently fitted with a truss-pin. The quantities of the reactions at A and $\overline{A}$ were determined by tests.

In one of the first experiments the members O_{10}, U_{17} and $\overline{O}_{10}$ were all of the same section, namely 2.88 cm². The yield point stress for these bars was $\sigma_s = 2.68$ t/cm² and the carring moment $M_s = 2.88 \cdot 50 \cdot 2.68 = 386$ cmt. Making no allowance for the dead weigth of the structure for 4 equal concentrated loads acting in point 14, 16, $\overline{16}$, $\overline{14}$ respectively the purely elastic reactions at the outer supports are equal to 0.418 P

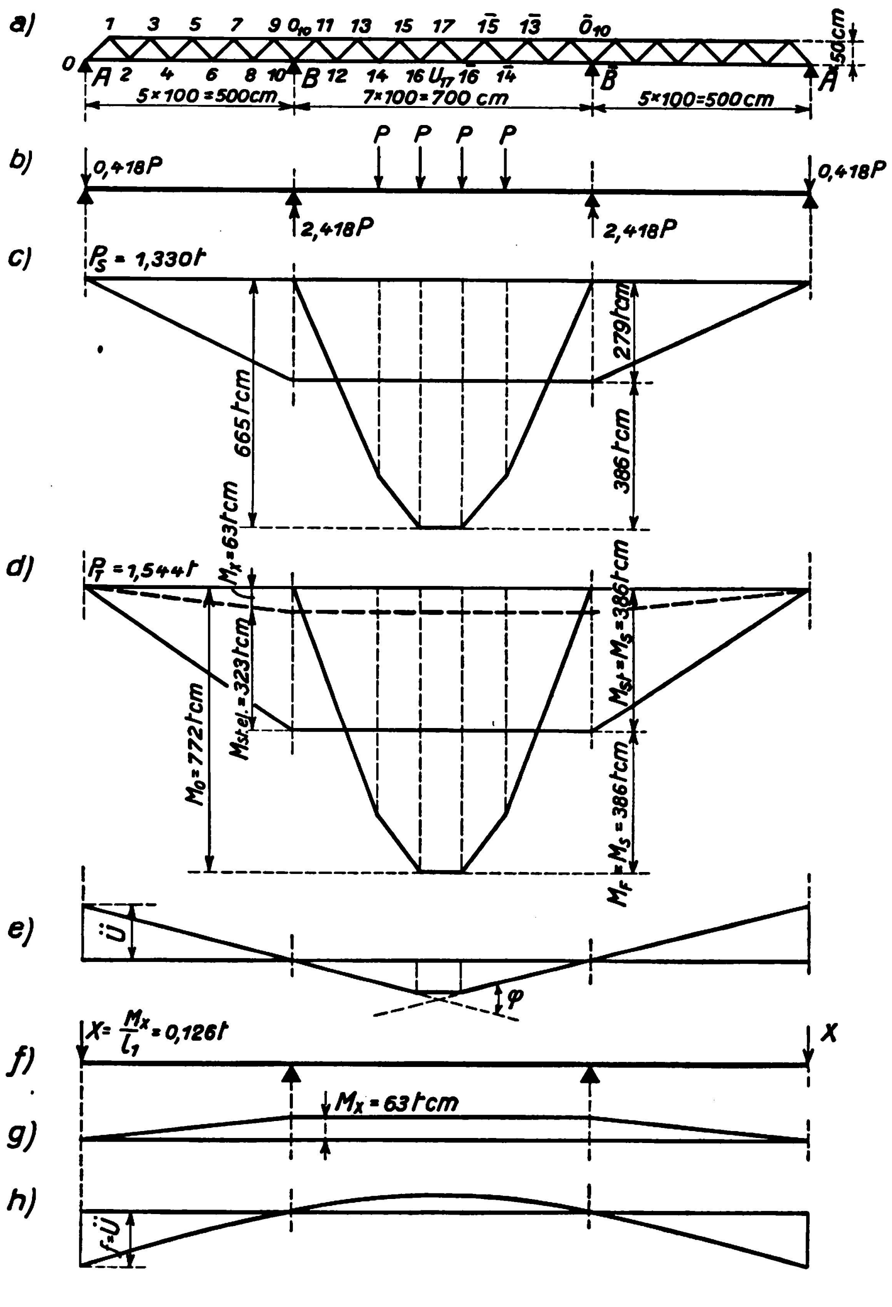

Fig. 29.

and hence those at the intermediate supports equal to 2.418 P. Accordingly the moments at those supports are $M_{st} = 0.418 \cdot 500$ P $= 209$ P and the maximum moment in the central span $M_F = (500 - 209)$ P $= 291$ P. The loads P_s causing the member U_{17} to begin to yield, are deduced from 291 $P_s = M_s = 386$ cmt to $P_s = 1.33$ t, see Fig. 29c. The loads P_T for which the members O_{10} and $\bar{O}_{10}$ begin also to yield are found to be $P_T = 1.544$ t based (Fig. 29 d) on $M_{st} = M_O - M_s = M_s$ i. e. $500 \cdot P_T = 2 \cdot 386$ cmt. The relations between M_{st}, M_F, P_s and P_T are given in Fig. 30 a. If the girder is released of its loads P_T we find permanent deformations in

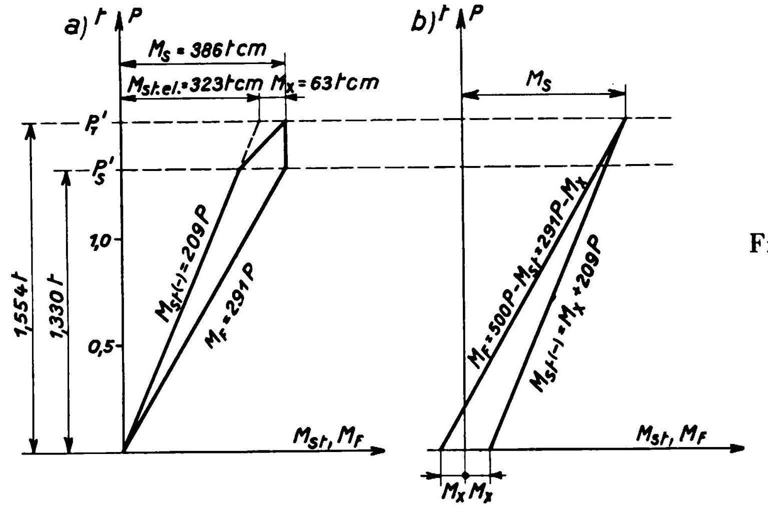

Fig. 30.

the lower chord as given in Fig. 29 e. The deflection line shows an angle φ under point 17, causing an elevation ü. Before actual reloading takes place, the ends of the girder have to be brought back first on to the bearings through the introduction of the forces X (Fig. 29 f). These forces create bending mo-

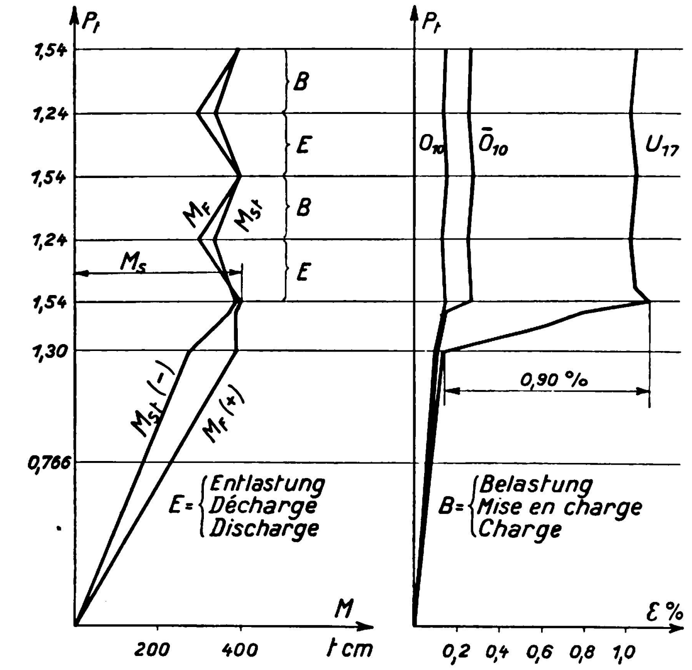

Fig. 31.

ments over the supports of $M_x = X \cdot l_1$, to which have to be added the moments $M_{st.el} = 209\ P_T = 323$ cmt produced by loading of the girder with the forces P_T. From $M_x + M_{st.el} = M_s$ follows that (Fig. 29 d) $M_x = 63$ cmt and $X = 0.126$ t. The deflection f at the girder end due to X must be equal to ü; with this condition we receive φ and the permanent deformation

Δs of the bar U_{17}, due to the loads P_T [Δs could alternatively be obtained from the deformations of the line A, B, 16, 17, $\overline{16}$, $\overline{B}$, $\overline{A}$]. A reloading of the girder produces the conditions laid down in Fig. 30b. The test results given in Fig. 7 of [18] are produced in Fig. 31. These values show good agreement with the values deduced from the interpretation of the tests (29 and 30), making no allowance, however, for the dead weight of the girder and assuming a frictionsless hinge in point 17.

Further tests described in [18] were for cases with I-bars having reduced cross sections for certain portions of these bars and for cases charged with heavier external loads than P_T. Further, the influence of subsidence of the supports on the carrying capacity was studied. A single lifting of the outer

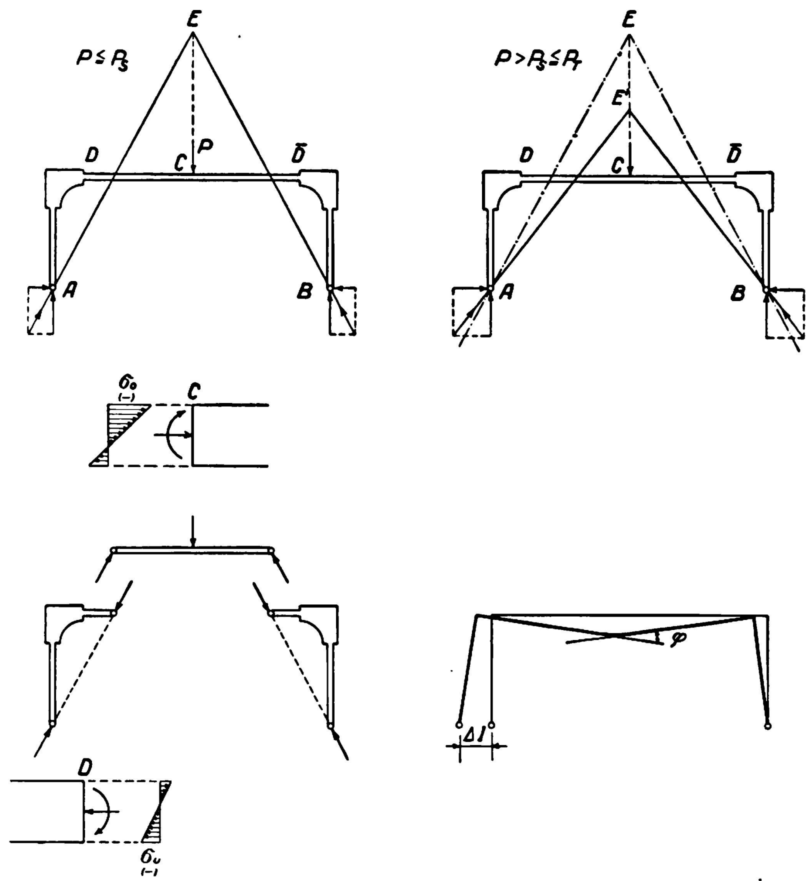

Fig. 32.

bearings did not impair the carrying capacity; but repeated lowering and lifting of the supports of the girder loaded with P_T will naturally be detrimental.

As regards the conclusions to be drawn from the experiments which still require to be continued, a reference is made to [18] p. 72.

It would be of particular interest to obtain some knowledge about the actual carrying capacity of continuous latticed girders whose critical members are weakened, e. g. in consequence of rivet holes.

G. Rectangular portal frame.

K. Girkmann reported in [19] on a test which he carried out and to which refers Fig. 32.

The frame structure AB with corners purposely overdimensioned received an increasing load P in mid-span of the brace $D\bar{D}$. First a pressure line AEB is established by the load P, giving a stress distribution in cross sections C and D as shown in Fig. 32. The maximum stress takes place in the upper extreme fibres of the cross section C (compression).

This stress reaches the yield point stress for a load P_s. For increasing loads, $P > P_s$, the elements of the brace near C will be deformed in such a way that on replacing one of the fixed bearings of the frame by a movable bearing a displacement of Δl will take place. This means that for loads $P > P_s$ a greater horizontal thrust will be established than expected according to the usual

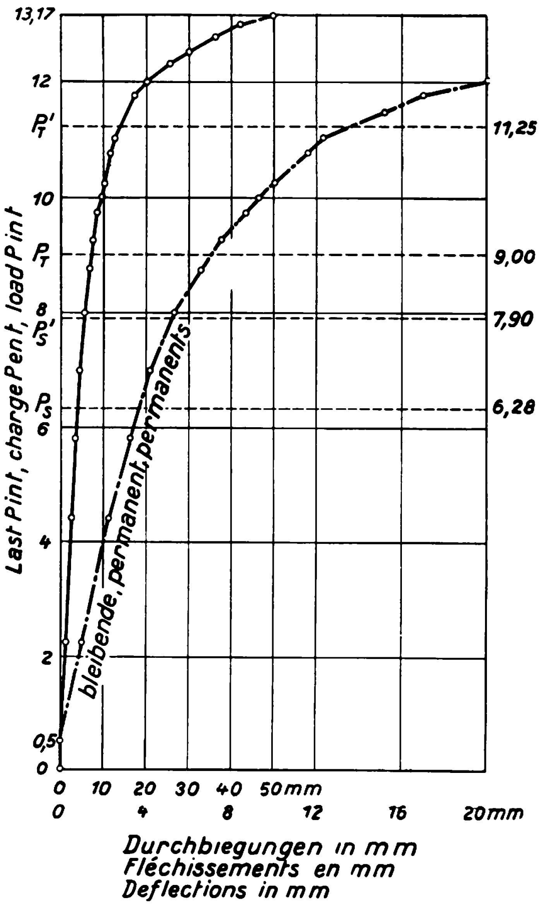

Fig. 33.

theory. The pressure line will be less steep. The frame starts to fail definitely if yield point stresses are obtained at the bottom of the cross section D. The carrying capacity can be calculated, with sufficient accuracy for practical purposes, by assuming that the pressure line passes in the centre between C and D; or more exactly between the core-points which are decisive for σ_o in C and σ_u in D. Introducing the respective cross sections into the calculation without making deductions for rivet holes we receive:

$P_{adm} = 2.88$ t for $\sigma_{zul} = 1.2$ t/cm^2; $P_s = 6.28$ t with stressing at one place only of $\sigma_s = 2.62$ t/cm^2 (on top of cross section C); $P_T = 9.00$ t the practical carrying capacity. The assumption is hereby made that cross section acts as a hinge immediately after attaining the yield stress at the topmost fibres.

The customary theory of elasticity allows for the frame under consideration a carrying capacity of 6.28 t only. The test has proved (see Fig. 33) that only from a load of P = 11.25 t upwards do the deformations in mid-span of the brace $D\bar{D}$ grow rapidly; therefore $P'_T = 11.25$ t and accordingly $P'_s = \sim P'_T \cdot \frac{P_s}{P_T} = \sim 11.25 \cdot \frac{6.28}{9.00} = 7.9$ t. Fracture occured, starting from a rivet hole in mid-span, at $P_v = 13.17$ t. For other observations made attention is drawn to details given in [19].

L i s t

of important treatises on the influence of ductility (plasticity) of building steel on the dimensioning of steel structures particularly such publications which refer to tests.

F. Bleich: La ductilité de l'acier. Son application au dimensionnement des systèmes hyperstatiques. *L'Ossature Métallique 3 (1934), p. 93.*

F. Bleich: La théorie et la recherche expérimentale en construction métallique. *L'Ossature Métallique 3 (1934), p. 627.*

H. Bleich: Über die Bemessung statisch unbestimmter Stahltragwerke unter Berücksichtigung des elastisch-plastischen Verhaltens des Baustoffes. *Bauingenieur 13 (1932), p. 261.*

[8] *F. Bohny:* Über die Verwendung von Nickelstahl im Brückenbau (see page 90 test with I-beam No 30). *Der Eisenbau 2 (1911), p. 79.*

[9] *J. E. Brik:* Über den Knickwiderstand der Druckgurte vollwandiger Balkenträger (contains informations about tests with simple beams). *Der Eisenbau 3 (1912), p. 351 und 4 (1913), p. 189, 192, 353.*

Eisenmann: Theorie und Statik plastischer Träger des Stahlbaues. *Stahlbau 6 (1933), p. 25. Erwiderung 6 (1933), p. 54.*

[16] *F. v. Emperger:* Versuche mit eingespannten Balken in Heft 5 der Mitteilungen über Versuche ausgeführt vom Eisenbetonausschuß des österreichischen Ingenieur- und Architekten-Vereins. *F. Deuticke, Leipzig und Wien 1917.*

[3] *J. Fritsche:* Die Tragfähigkeit von Balken aus Stahl mit Berücksichtigung des plastischen Verformungsvermögens. *Bauingenieur 11 (1930), p. 851, 873, 888.*

J. Fritsche: Die Tragfähigkeit von Balken aus Baustahl bei beliebig oft wiederholter Belastung. *Bauingenieur 12 (1931), p. 827.*

[5] *J. Fritsche:* Grundsätzliches zur Plastizitätstheorie. *Stahlbau 9 (1936), p. 65.*

[19] *K. Girkmann:* Über die Auswirkung der „Selbsthilfe" des Baustahls in rahmenartigen Stabwerken. *Stahlbau 5 (1932), p. 121.*

[14] *O. Graf:* Über Dauerversuche mit I-Trägern aus St. 37. *Stahlbau 7 (1934), p. 169.*

[18] *G. Grüning & E. Kohl:* Tragfähigkeitsversuche an einem durchlaufenden Fachwerkbalken aus Stahl. *Bauingenieur 14 (1933), p. 67.*

Martin Grüning: Die Tragfähigkeit statisch unbestimmter Tragwerke aus Stahl bei beliebig häufig wiederholter Belastung. *Broschüre Berlin 1936.*

[2] *M. Grüning-Kulka* und andere: Zuschriften an die Schriftleitung betreffend Plastizität *Bautechnik 6 (1928), p. 274.*

[4] *F. Hartmann:* Die Formänderungen einfacher und durchlaufender Stahlträger. Mit einem Versuch.
Schweiz. Bauzeitung 101 (1933), p. 75.

F. Hartmann: Über die Erhöhung der zulässigen Inanspruchnahme von stählernen Brücken.
Zeitschrift des Österr. Ingenieur- und Architekten-Vereins 1935, Heft 21/22 und 23/24.

A. S. Joukoff: Principes d'application de la plasticité au calcul des constructions métalliques hyperstatiques.
L'Ossature Métallique 3 (1934), p. 379.

F. Kann: Der Momentenausgleich durchlaufender Traggebilde im Stahlbau.
Broschüre, Verlag de Gruyter & Co. 1932.

F. Kann: Rechnerische Untersuchungen über die Größe des Fließbereiches in stählernen Durchlaufbalken unter Berücksichtigung des Momentenausgleichs.
Stahlbau 5 (1932), p. 105. Berichtigung (1932), p. 160.

[15] *G. v. Kazinczy:* Kisérletek befalozott tartékkal (Tests with fixed-end beams.)
Betonszemle 2 (1914), Nr. 5, 6, 7.

G. v. Kazinczy: Bemessung von statisch unbestimmten Konstruktionen unter Berücksichtigung der bleibenden Formänderungen.
Internationaler Kongreß für Eisenbau, Liége September 1930.

[13] *G. v. Kazinczy:* Statisch unbestimmte Tragwerke unter Berücksichtigung der Plastizität.
Stahlbau 4 (1931), p. 58.

G. v. Kazinczy: Die Weiterentwicklung der Plastizitätslehre.
Sonderdruck aus dem 12. Jahrgang der „Technica", Budapest 1931.

G. v. Kazinczy: Die Bemessung unvollkommen eingespannter Stahl I-Deckenträger unter Berücksichtigung der plastischen Formänderungen.
2. Band der Abhandlungen der Internationalen Vereinigung für Brückenbau und Hochbau, Zürich 1934.

N. C. Kist: Die Zähigkeit des Materials als Grundlage für die Berechnung von Brücken, Hochbauten und ähnlichen Konstruktionen aus Flußeisen.
Der Eisenbau 11 (1920), p. 425.

N. C. Kist: Ductility as a base for design-computation of steel bridges and structures instead of proportionality of stress and strain.
La Technique des Travaux, Liége September 1930.

N. C. Kist: La Déformation en palier de l'acier substituée à la loi de Hooke comme base de calcul de la résistance des ponts et charpentes métalliques.
Science et Industrie. Edition: Construction et Travaux Publics. März 1933.

O. Knackstedt: Beitrag zur Ermittlung der wirklichen Tragfähigkeit statisch unbestimmter Vollwandträger aus Stahl unter Berücksichtigung der plastischen Verformung.
Dissertation, Braunschweig 1932.

O. Lienau: Der Einfluß der Streckung auf die Tragfähigkeit durchlaufender Eisenträger.
Zeitschrift Der Schiffbau 29 (1928), p. 532.

[11] *Maier-Leibnitz:* Beitrag zur Frage der tatsächlichen Tragfähigkeit einfacher und durchlaufender Balkenträger aus Baustahl St. 37 und aus Holz.
Bautechnik 6 (1928), p. 11, 27.

Maier-Leibnitz: Diskussionsbeitrag im Bericht über die 2. Internationale Tagung für Brückenbau und Hochbau.
Wien 1928, p. 257.

[1] *Maier-Leibnitz:* Versuche mit eingespannten und einfachen Balken von I-Form aus St. 37.
Bautechnik 7 (1929), p. 313. Berichtigung (1929), p. 366.

Maier-Leibnitz: Artikel: „Zulässige Beanspruchung" in Luegers Lexikon der Gesamten Technik und ihrer Hilfswissenschaften.
Luegers Lexikon der gesamten Technik ca. 1930.

[17] *Maier-Leibnitz:* Frage der tatsächlichen Tragfähigkeit durchlaufender vollwandiger Balken aus Baustahl mit drei Feldern.
Stahlbau 9 (1936).

[7] *H. F. Moore:* The strength of I-beams in flexure (consains references to other publications about tests with simple beams).
Bulletin Nr. 68 der University of Illinois, Engineering Experiment Station vom 1. September 1913.

[10] *K. A. Müllenhoff:* Versuche an schmiedeeisernen Blechträgern (references to tests of F. Mc. Kibben der Lehigh University on simple beams).
Der Eisenbau 4 (1913), p. 157.

[12] *J. H. Schaim:* Der durchlaufende Träger unter Berücksichtigung der Plastizität.
Stahlbau 3 (1930), p. 13.

E. Siebel und *H. F. Vieregge:* Über die Abhängigkeit des Fließbeginns von Spannungsverteilung und Werkstoff.
Mitteilungen aus dem Kaiser-Wilhelm-Institut für Eisenforschung 1934, Band XVI, Lieferung 21.

[6] *F. Stüssi* und *C. F. Kollbrunner:* Beitrag zum Traglastverfahren.
Bautechnik 13 (1935), p. 264.

F. Stüssi: Sicherheit statisch unbestimmter Fachwerke bei Veränderung einzelner Stabquerschnitte. Beitrag zur wirtschaftlichen Verstärkung statisch unbestimmter Fachwerkträger mit geringsten Eingriffen.
Bautechnik 9 (1931), p. 603.

F. Stüssi: Aktuelle baustatische Probleme der Konstruktionspraxis.
Schweiz. Bauzeitung 1935, Sonderdruck.

Summary.

The paper gives a summary of loading tests carried out with different types of structural elements. With some of these tests the yield limit is exceeded. It can be demonstrated in every case that the load P_s is not decisive for the carrying capacity, simply because on application of the theory of elasticity, the yield limit is reached somewhere in the structure. In fact a higher value P_T is reached for the carrying capacity. To determine the actual carrying capacity, a procedure is given (simplified hypothesis of interpretation), which supplies sufficiently accurate values for practical purposes. The procedure also serves to interpret the results of the tests. If necessary, the interpretation of these results and the mode of calculation for the determination of P_T can still be refined.